UNIVERSITY OF VAASA
FACULTY OF TECHNOLOGY
TELECOMMUNICATIONS ENGINEERING

Ruifeng Duan

OPTIMIZING RADIO RESOURCE MANAGEMENT IN VERY BAD CHANNEL CONDITIONS

Master's thesis for the degree of Master of Science in Technology submitted for inspection in Vaasa, 17th of May, 2008.

Supervisor D.Sc. (Tech.) Mohammed Salem Elmusrati

Instructor D.Sc. (Tech.) Mohammed Salem Elmusrati

ACKNOWLEDGEMENTS

First of all, I am deeply grateful to my advisor, Prof. Mohammed Elmusrati, for his endless support, guidance, and encouragement throughout this thesis. His friendly and patient attitude, creativity, depth of knowledge helped me to have a great educational experience at Telecommunication Engineering Group (TEG).

I would also like to extend my appreciation and thanks to Dr. Petteri Mannersalo who was an acting professor in TEG during 2006-2007, influenced my research positively.

In addition, I would like to thank Mr. Reino Virrankoski for bringing me quite useful knowledge in wireless communications and networks. I would like to thank Mr. Veli-Matti Eskonen and Juha Miettinen for making a friendly research environment.

Moreover, I would like to thank all my friends in TEG, Mr. Tobias Glocker, Lu Zhonglei, Teemu Ahonen, and Xiang Chao, for their help, discussion, and the fun we had made together. And I would like to thank all my friends, here at University of Vaasa and elsewhere.

Finally, my warmest thanks go to my family for the lifelong encouragement, support and love.

This research was supported by Telecommunication Engineering Group, University of Vaasa.

TABLE OF CONTENTS

ABBREVIATIONS AND ACRONYMS

3G	Third Generation Mobile Communication System
4G	Fourth Generation Mobile Communication System
AC	Admission Control
BPSK	Binary Phase Shift Keying
BS	Base Station
CDF	Cumulative Distribution Function
CDMA	Code Division Multiple Access
DCP	Distributed Power Control
DCPC	Distributed Constrained Power Control
FER	Frame Error Rate
HO	Handover
IEEE	Institute of Electrical and Electronics Engineers, Inc.
ISI	Inter Symbol Interference
LoS	Line of Sight
MS	Mobile Station
PDF	Probability Density Function
QPSK	Quadrature Phase-Shift Keying
QAM	Quadrature Amplitude Modulation
R-REQCH	Reverse Request Channel
RMS	Root Mean Square
RRM	Radio Resource Management
SINR	Signal to Interference and Noise Ratio
TPC	Transmit Power Control
UE	User Equipment
WCDMA	Wideband Code Division Multiple Access
WiMAX	Worldwide Interoperability for Microwave Access
WLAN	Wireless Local Area Networks
WSN	Wireless Sensor Networks

SYMBOLS

B_s	Baseband Signal Bandwidth
D_s	Doppler spread
G_r	Receiver Antenna Gain
G_t	Transmitter Antenna Gain
λ	Wavelength
P_t	Transmit Power
$P_r(d)$	Received Power at Distance d
T_c	Channel Coherence Time
T_s	Symbol Duration
τ	Time Delay
$\overline{(\cdot)}$	Expectation
μ	Mean Value
σ^2	Variance

UNIVERSITY OF VAASA
Faculty of technology
Author: Ruifeng Duan
Topic of the Thesis: Optimizing Radio Resource Management in Very Bad Channel Conditions
Supervisor: Mohammed Elmusrati
Instructor: Mohammed Elmusrati
Degree: Master of Science in Technology
Department: Department of Computer Science
Degree Programme: Degree Programme in Information Technology
Major of Subject: Telecommunication Engineering
Year of Entering the University: 2006
Year of Completing the Thesis: 2008
Pages: 106

ABSTRACT

Radio resource management is one of the most important parts of modern multi-user wireless communication systems. The main reason for this importance comes from the fact that the radio resources, such as bandwidth and power, are scarce. For instance, UMTS systems use 5MHz bandwidth for voice as well as data services. The optimum usage of the radio resource guarantees the highest efficient utilization of wireless networks. To optimize the radio resources, the transmitters need to estimate the channel conditions. This channel estimation is done by using pilot signal from the receiver. There are usually small delays between the measurements and the radio resource allocation. When the channel is highly correlated, this delay will not affect the performance, because the channel will not be significantly changed between the time of measurement and the time of transmission. However, if the mobile speed is high or the channel is very high dynamic, the correlation becomes very low. This is due to the time-varying nature of the channel. We call channels with very low correlation in time as bad condition channels.

In this thesis we discuss this extremely important topic. The tools for analyzing bad condition channels are also proposed and discussed. Two power control algorithms to mitigate the low correlation of channels have been proposed. Our algorithms are validated through several simulations.

KEYWORDS:

Wireless Communication, Time-varying Channel, Doppler Shift, Correlation, Fading, Radio Resource Management, Power Control

1. INTRODUCTION

Wireless communications as the fastest growing segment of the communications industry has experienced a tremendous growth spurt in the past decade. Thus in order to cope with the increasing demands for providing high-speed and high-quality services, wireless communication has experienced a rapid improvement. A variety of new wireless technologies, new standards, more efficient algorithms, and so on, have been emerging, for instance, modern cellular radio systems, wireless local area networks (WLAN), wireless Ad hoc networks, wireless sensor networks (WSN), and others. The new generations of cellular networks, third generation (3G), fourth generation (4G), and beyond, are designed not only for voice communications but also for multimedia communications. However, many technical challenges remain in designing robust wireless networks, for instance, the interference among mobile users. Therefore, we have to figure out the problems mathematically. In my thesis there are many simple examples and figures used to explain and discuss them.

Thus in the first part of this work we will introduce the essential characteristics of time-varying wireless channels. The time-varying characteristics of mobile channels as well as the time delays between the channel measurements and resource allocation will reduce the performance of current radio resource management algorithms. In this part, we can obtain some helpful information for further study. After this, we will know why we have so many problems, what factors cause these problems, how the radio signals are transmitted, and others. Some required tools from mathematics and stochastic process will be provided. These tools are used to analyze the mobile channels.

Besides the radio channel analysis, next we will introduce the radio resource management part, especially on power control schemes. This part is also a very important part of this thesis. For instance, we will show why only the mobile with better link quality can be served if there is no proper power control policy. Then we present more advanced power control schemes and algorithms.

Finally, we will propose two power control/allocation schemes for bad channel conditions. We mean by bad channel conditions that channels with low time correlation. This low correlation results due to the high dynamics of channels, or due to high mobile speed. Then we propose a random power allocation scheme for uncorrelated Rician fading channels.

2. LARGE-SCALE PATH LOSS AND SHADOWING

In this chapter, we introduce the effects of the large-scale distance-dependent attenuations in the average signal power, and diffraction and shielding phenomena. These are known as large-scale path loss and shadowing respectively. First, the radio communication channel characteristics are presented. Second, the radio wave propagation as well as the ray tracing models will be discussed. Last, we will show the path loss models and log-normal shadowing.

2.1 Radio Communication Channel

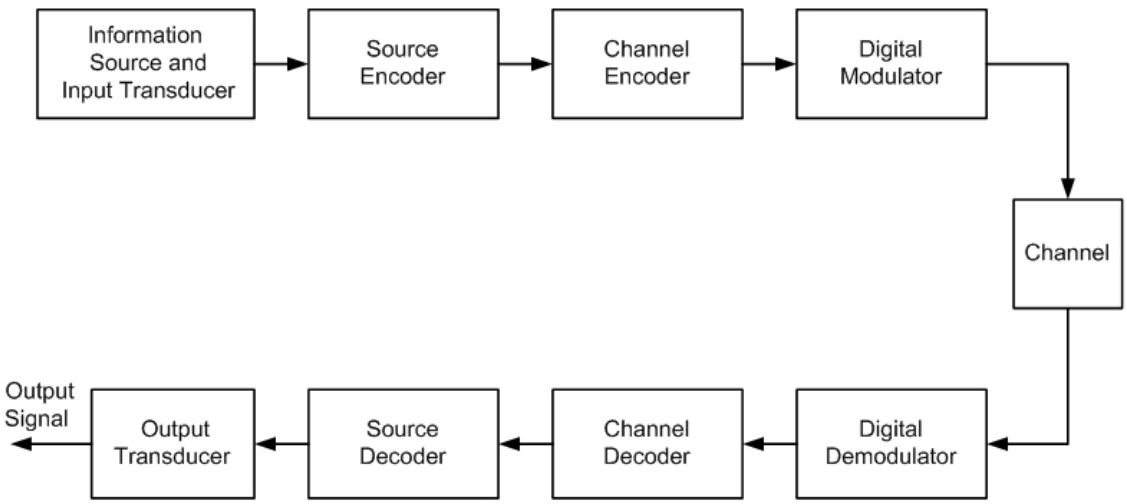

Figure 2.1: Basic Elements of a Digital Communication System (Proakis 2000: 2).

Fig. 2.1 indicates a block diagram of a digital communication link. From the figure we can find that the communication channel plays a key role in signal propagation between the transmitter and the receiver (Proakis 2000: 2). In practice, the physical channels can

be wired cables, optical fibers, or free space through which the radio wave signal carrying the information is radiated and received by antennas. In addition, there are also other transmission media, such that data storage media, underwater acoustic channels. Whatever the physical medium transmitting the information, the obvious feature is that the transmitted signal will be corrupted by a variety of interference sources, for instance, additive thermal noise, man-made noise, atmospheric noise, and etc. (Proakis 2000: 21).

2.2 Introduction to Radio Wave Propagation

The radio channel places fundamental limitations on the performance of wireless communication systems. The purpose of a radio communication system is to transmit information from transmitters to receivers. The radio waves propagating in free space will suffer reflection, diffraction, and scattering. In the urban environment where there is no direct line- of-sight path between the transmitter and receiver the radio wave will suffer severe diffraction loss. Also the radio wave will be reflected by various objects such that they will pass different paths of varying lengths. In consequence, the transmitted signal will experience multipath fading, that is, the received signal will experience construction or destruction when the relative location of the mobile to the transmitter, or the near vicinity along the transmission path changes. So the wireless channels are random and not easy to analyze and make prediction like the wired channels. As a result, modeling the radio channel is done in a statistical fashion (Goldsmith 2005; Parsons 1999; Proakis 2000; Rappaport 2002; Sklar 2001).

Fig. 2.2 shows an overview of fading-channel manifestations, which are first characterized into two types of fading effects, large-scale fading and small-scale fading (Sklar 2001: 948). Large-scale fading can be defined as the average power loss in the transmission of the signal over large distances. This phenomenon is mainly due to prominent terrain contours (hills, forests, building, etc.) between the transmitter and the receiver (Sklar 2001: 950). According to the statistics of large-scale fading, the path loss can be expressed by a function of distance which is often described in terms of a mean-

path loss (*n*th-power law) and a log-normally distributed variation about the mean (Sklar 2001: 951). On the other hand, small-scale fading refers to the dramatic changes in amplitude and phase of the received signal, occurring because of small (as small as a half wavelength) variations in the distance between the transmitter and the receiver. Small-scale fading manifests itself by means of two different mechanisms: the time spreading of the signal and the time variance of the channel, the latter due to spatial changes of the channel itself (movement of the transmitter and/or receiver, and also movements of the surrounding objects) (Sklar 2001: 951). For small-scale fading, if the number of multiple paths is large and there is no Line of Sight (LoS) which is a direct path from transmitter to receive, then the envelope of the received signal can be statistically described by a Rayleigh distribution, otherwise, if LoS is present, the envelope is Rician distributed (Parsons 1999:114; Rappaport 2002: 220). Also Nakagami-m distribution can be used to model small-scale fading through utilizing different values of *m* to model different cases, Rayleigh, Rician, worse than Rayleigh (Aulin 1981; Nakagami 1960; Tjhung & Chai 1999).

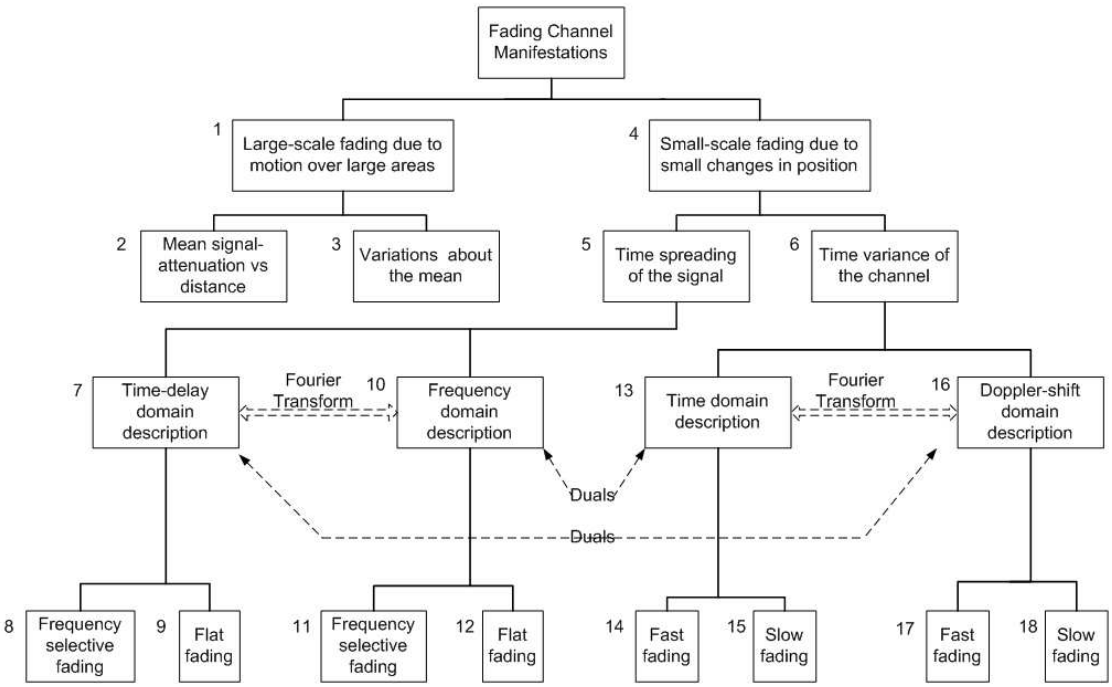

Figure 2.2: Fading Channel Manifestations (Sklar 2001: 948).

Path loss is the large-scale distance-dependent attenuation in the average signal power, which is used to separate the small-scale variation from the large-scale shadowing effects (Sklar 2001: 951). There are three basic propagation mechanisms impacting signal propagation in a mobile communication system as following (Rappaport 2002: 113-114):

• Reflection occurs under the situation that a propagating electronic wave impinges upon a smooth surface with very large dimensions compared to the signal wavelength.

• Diffraction occurs when the radio path between the transmitter and the receiver is obstructed by a dense body with larger dimensions relative to the signal wave or by a surface with sharp edges. Then the secondary waves will present around the obstacle, even behind it. This phenomenon is also termed shadowing that the wave can reach the obstructed receiver.

• Scattering occurs when the a radio wave reaches on either a large and rough surface or surfaces with smaller or on the order of dimensions compared to wave length. For this case, the energy of the radio wave is spread out or reflected in all directions. Practically, lampposts, street signs, foliage, etc. will result in scattering.

2.3 Free Space Propagation

The free space propagation model predicts the received signal strength when a clear, direct LoS path exists between the transmitter and the receiver, for instance, satellite communication systems and microwave LoS radio links (Parsons 1999: 130; Rappaport 2002: 115). In this case, the received power at the receiver antenna d meters away from the transmitter is given by the Friis free space equation.

$$P_r(d) = \frac{P_t G_t G_r \lambda^2}{(4\pi)^2 d^2 L} \quad , \tag{2.1}$$

where P_t is the transmit power, $P_r(d)$ is the received power at distance d, G_t is the transmitter antenna gain, G_r is the receiver antenna gain, d is the distance between the transmitter and the receiver in meters, L is the system loss factor not related to propagation ($L \geq 1$) , and λ is the wavelength in meters. For simplicity, we assume that there is no loss in the system hardware, such that L = 1, then equation (2.1) comes to

$$P_r(d) = \frac{P_t G_t G_r \lambda^2}{(4\pi)^2 d^2} \quad . \tag{2.2}$$

The antenna gain is defined as

$$G = \frac{4\pi A_e}{\lambda^2} \ , \tag{2.3}$$

where A_e is the effective aperture of the antenna, and λ is the wavelength defined as

$$\lambda = \frac{c}{f}, \tag{2.4}$$

where f is the carrier frequency in Hertz and c is the speed of light in meters/s. The propagation loss or path loss represents the transmitted signal attenuation. The free-space path loss is expressed in dB scale as

$$PL(dB) = 10log\frac{P_t}{P_r} = -10log\left[\frac{G_t G_r \lambda^2}{(4\pi)^2 d^2}\right] \tag{2.5}$$

When the antennas are isotropic, that is, the antenna gains are equal to 1. Then the path loss becomes

$$PL(dB) = 10log\frac{P_t}{P_r} = -10log\left[\frac{\lambda^2}{(4\pi)^2 d^2}\right] \quad (2.6)$$

2.4 Ray Tracing Models

This section discusses two simple ray tracing models. The first one is a simple two-path model predicting signal variation resulting from a reflected ray interfering with the LoS path. This model characterizes signal propagation in isolated areas with few reflectors, such as rural roads or highways (Goldsmith 2005: 48). Secondly, diffraction is discussed, which illustrates the phenomenon that the radio waves propagate around the curved surface of the earth, beyond the horizon and to propagate behind obstructions.

2.4.1 Two-Path Model

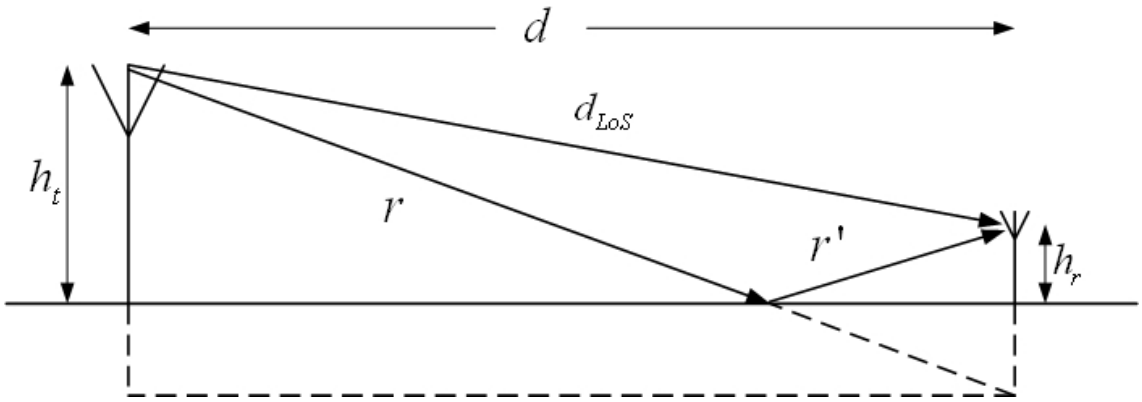

Figure 2.3: Two-path model.

There are two propagation signals through two paths, as illustrated in Figure 2.3, one is the dominant one and the other is a single ground reflection which does not means that only one signal exists but reflected signal dominates the multipath effect. The received signal is a combination of these two components. The received LoS component is

determined from the free-space propagation loss formula, given by (Goldsmith 2005: 50; Rappaport 2002: 120-125):

$$r_{LoS}(t) = \Re\left\{ u(t) \frac{\lambda\sqrt{G} e^{-j(2\pi d_{LoS}/\lambda)}}{4\pi d_{LoS}} e^{j2\pi f_c t} \right\} \tag{2.7}$$

where d_{LoS} is the length of the LoS path and G is the product of the transmit and receive antenna field radiation patterns. The reflected ray is illustrated in Figure 2.3 by paths, r and r'. Then the combined signal at the receiver for the two-path model comes to

$$r_{2\,path}(t) = \Re\left\{ \frac{\lambda}{4\pi} \left[\frac{\sqrt{G}u(t)e^{-j(2\pi d_{LoS}/\lambda)}}{d_{LoS}} + \frac{R\sqrt{G}u(t-\tau)e^{-j(2\pi(r+r')/\lambda)}}{r+r'} \right] e^{j2\pi f_c t} \right\} \tag{2.8}$$

where $\tau = (r + r' - d_{LoS}) / \lambda c$ is the time delay of the reflected ray and R is the reflection coefficient. Then the receiver signal power of the two-ray model approximately is

$$P_r = P_t \left(\frac{\lambda}{4\pi} \right)^2 \left| \frac{\sqrt{G}}{d_{LoS}} + \frac{R\sqrt{G} e^{-j2\pi(r+r'-d_{LoS})/\lambda}}{r+r'} \right|^2 \tag{2.9}$$

By using geometry showed in Fig. 2.3, we can obtain that the distance difference between the LoS path and the reflected path is

$$\begin{aligned} \Delta d &= r + r' - d_{LoS} \\ &= \sqrt{(h_t + h_r)^2 + d^2} - \sqrt{(h_t - h_r)^2 + d^2} \\ &= d\left(\sqrt{1 + \frac{(h_t + h_r)^2}{d^2}} - \sqrt{1 + \frac{(h_t - h_r)^2}{d^2}} \right) \end{aligned} \tag{2.10}$$

When $d \gg h_t, h_r$, we have

$$\sqrt{1+\frac{(h_t+h_r)^2}{d^2}} \approx 1+\frac{(h_t+h_r)^2}{2d^2}$$
$$\sqrt{1+\frac{(h_t-h_r)^2}{d^2}} \approx 1+\frac{(h_t-h_r)^2}{2d^2} \tag{2.11}$$

Then equation 2.10 comes to

$$\begin{aligned}\Delta d &= d\left(1+\frac{(h_t+h_r)^2}{2d^2}-1-\frac{(h_t-h_r)^2}{2d^2}\right) \\ &= \frac{2h_t h_r}{d}\end{aligned} \tag{2.12}$$

For $d \gg h_t, h_r$, then we have $r + r' \approx d_{LoS} \approx d$, and $R = -1$(Goldsmith 2005: 31). We also have $e^{-jx} \approx 1 - jx,$ for x $\ll 1$. Therefore equation 2.9 becomes

$$\begin{aligned}P_r &\approx P_t\left(\frac{\lambda}{4\pi}\right)^2\left|\frac{\sqrt{G}}{d}-\frac{\sqrt{G}e^{-j4\pi h_t h_r/d\lambda}}{d}\right|^2 \\ &= P_t\left(\frac{\lambda}{4\pi}\right)^2\frac{G}{d^2}\left|1-e^{-j4\pi h_t h_r/d\lambda}\right|^2 \\ &\approx P_t\left(\frac{\lambda}{4\pi}\right)^2\frac{G}{d^2}\left|j\frac{4\pi h_t h_r}{d\lambda}\right|^2 \\ &= \frac{G h_t^2 h_r^2}{d^4}P_t\end{aligned} \tag{2.13}$$

In consequence, the received signal power $P_r \propto \frac{1}{d^4}$.

2.4.2 Diffraction

Diffraction allows radio waves to propagate around the curved surface of the earth, beyond the horizon and behind obstructions. Although the deeper a receiver moves into the shadowed region the weaker the signal field strength becomes, we also can obtain a useful diffracted signal. This phenomenon can be explained by Huygen's principle showed in Fig. 2.4 (Parsons 1999: 33; Rappaport 2002: 120-125), which shows that all points on a wavefront can be considered as point sources for the production of secondary wavelets combining to product a new wavefront in the direction of propagation. The phenomenon of propagation of secondary wavelets into a shadowed region causes diffraction. In consequence, the field strength of a diffracted wave in the shadowed region is the vector sum of the electronic field components of all the secondary wavelets in the space around the obstacles (Parsons 1999: 34-35). Next we will illustrate a basic model used to analyze the wave diffraction.

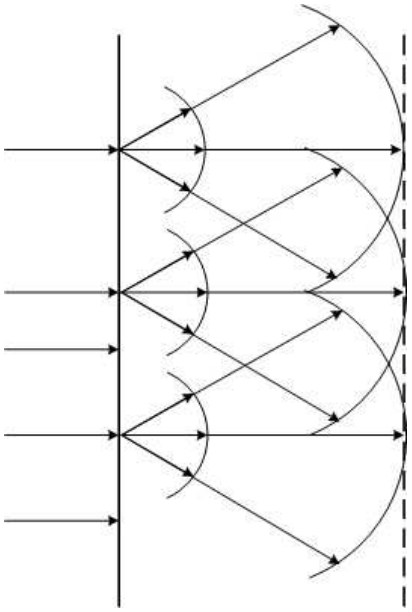

Figure 2.4: Huygen's principle applied to propagation of plane waves.

Knife Edge Diffraction Model

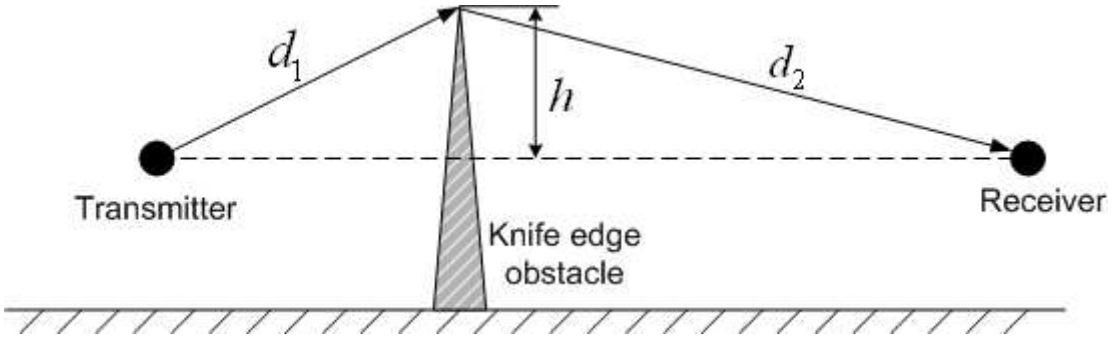

Figure 2.5: Knife Edge Diffraction.

When shadowing is caused by a single object, the attenuation caused by diffraction can be estimated by a knife-edge diffraction model (Rappaport 2002: 129-130). As showed in Fig. 2.5, the receiver is located in the shadowed region. Let $d_1 + d_2$ be travel distance of the diffracted signal, and h be the obstructing effective height. Also assume that $h << d_1$, d_2 and $h >> \lambda$, where λ is the wave length. Then geometrically, the *excess path length* Δd, which is the difference between the diffracted path and the direct one, becomes

$$\Delta d = \frac{h^2}{2}\frac{(d_1 + d_2)}{d_1 d_2} \tag{2.14}$$

The corresponding phase difference between the diffracted signal and the direct one is given by

$$\Delta\phi = \frac{2\pi\Delta d}{\lambda} = \frac{2\pi}{\lambda}\frac{h^2}{2}\frac{(d_1 + d_2)}{d_1 d_2}. \tag{2.15}$$

Let

$$\nu = h\sqrt{\frac{2(d_1 + d_2)}{\lambda d_1 d_2}} \tag{2.16}$$

which is defined as **Fresnel-Kirchoff diffraction parameter** (Rappaport 2002: 126-128). Then the phase difference can be simplified to

$$\Delta\phi = \frac{\pi}{2}\nu^2 . \tag{2.17}$$

However, it is quite complexed to compute this diffraction path loss, for Huygen's principle, Fresnel zones, and also the complex Fresnel integral should be used (Rappaport 2002: 126-128). Lee (1982: 140) presented approximations for knife-edge diffraction path loss relative to LoS path loss as

$$L_\nu(dB) = \begin{cases} 0, & \nu \le -1 \\ 20log(0.5 - 0.62\nu), & -1 \le \nu \le 0 \\ 20log(0.5e^{(-0.95\nu)}), & 0 \le \nu \le 1 \\ 20log(0.4 - \sqrt{0.1184 - (0.38 - 0.1\nu)^2}), & 1 \le \nu \le 2.4 \\ 20log(\frac{0.225}{\nu}), & 2.4 \le \nu \end{cases} \tag{2.18}$$

Then the received diffracted signal for knife-edge diffraction model is as follow

$$r(t) = \Re\left\{L_\nu\sqrt{G_d}\,u(t-\tau)e^{-j2\pi((d_1+d_2)/\lambda - f_c t)}\right\} \tag{2.19}$$

where G_d is the antenna gain, f_c is the carrier frequency, τ is the diffracted signal delay relative to the LoS one, and $u(t)$ is the complex envelope or complex lowpass equivalent signal of transmitted signal.

Here the basic models for diffraction phenomenon are presented. Please refer to (Goldsmith 2005; Lee 1982; Parsons 1999; Rappaport 2002) for the other models which are used to analyze the diffraction cases, such as double knife-edge diffraction, multiple knife-edge diffraction, Lee's macrocell model and etc..

2.5 Simplified Path Loss Model

For analyzing the path loss, there are many empirical path loss models developed, for instance, Okumura model, Hata model, COST 231 Extension to Hata model, Piecewise Linear model, and others (Goldsmith 2005: 70; Rappaport 2002: 138-140; Lee 1982: 150). However, it is quite difficult to model path loss characteristics accurately in a complex environment because of the complexity of signal propagation. Practically, a simple model is used to obtain the essential characteristic information of the path loss in a complicated case. The average large-scale path loss commonly used for system design is a function of distance by using a path loss exponent (Rappaport 2002: 138),

$$\overline{PL}(d) \propto (\frac{d}{d_0})^n \quad , \tag{2.20}$$

or in dB scale

$$\overline{PL}(dB) = \overline{PL}(d_0) + 10n\log(\frac{d}{d_0}) \tag{2.21}$$

where n is the path loss exponent stating the path loss increasing rate with the distance, d_0 is a reference distance for the antenna far-field (Goldsmith 2005) or the close-in reference distance determined from measurements close to the transmitter (Rappaport 2002: 140), d is the distance between the transmitter and the receiver. And $\overline{(\cdot)}$ in equation (2.20) and (2.21) means the overall average for all possible path loss for a given distance d. The path loss exponent n is an important factor for this path loss

model whose values are given as below depending on various propagation environments (Lee 1982: 177; Rappaport 2002: 142).

Table 2.1: Path Loss Exponents for Different Environments

Environment	**Path Loss Exponent, n**
Free Space	2
Urban area cellular radio	2.7 to 3.5
Shadowed urban cellular radio	3 to 5
In building line-of-sight	1.6 to 1.8
Obstructed in building	4 to 6
Obstructed in factories	2 to 3

2.6 Log-normal Shadowing

A signal transmitted through a wireless channel will typically experience random variation due to blockage from objects in the signal path, giving rise to random variations of the received power at a given distance. Such variations are also caused by changes in reflecting surfaces and scattering objects. Thus, a model for the random attenuation due to these effects is also needed. Since the location, size, and dielectric properties of the blocking objects as well as the changes in reflecting surfaces and scattering objects that cause the random attenuation are generally unknown, statistical models must be used to characterize this attenuation. The most common model for this additional attenuation is log-normal shadowing. This model has been confirmed empirically to accurately model the variation in received power in both outdoor and indoor radio propagation environments (Rappaport 2002: 139-140).

$$PL(d)(dB) = \overline{PL}(d_0) + X_\sigma = \overline{PL}(d_0) + 10n\log(\frac{d}{d_0}) + X_\sigma$$

3. SMALL-SCALE FADING AND MULTIPATH

The transmission path between the transmitter and the receiver can vary from simple line-of-sight to multipath resulting in the random characteristics. As what are illustrated previously, path loss is the large-scale distance dependent attenuation in the average signal power, and shadowing is caused by diffraction and shielding phenomena. While multipath fading is the rapid fluctuation in the received signal power caused by the constructive and destructive addition of the received multipath signals. These multipath waves propagate through different paths with different delays from the transmitter to the receiver. These effects are explained in more detail in the following sections.

3.1 Basic Information about Probability and Stochastic Processes

The probability theory and stochastic processes play an important role in studying digital and wireless communication systems, which is utilized to analyze the random variations mathematically. In the next section, we present some basic information about the probability and stochastic processes utilized to analyze the mobile fading channels. For the details illustrated in this section, please refer to (Papoulis 1965).

3.1.1 Characteristic Function

Characteristic function, $\Phi_X(\omega)$, of a random variable X is defined as

$$\Phi_X(\omega) = E(e^{j\omega X}) = \int_{-\infty}^{\infty} e^{j\omega x} f(x) dx \tag{3.1}$$

where $E(\cdot)$ denotes expectation, and $j = \sqrt{-1}$. From equation 3.1 we can find that characteristic function has two main advantages: first, $\Phi_X(\omega)$ is finite for all random

variables X and all real numbers ω; second, it is the Fourier transform (with a reversal in sign) of probability density function (PDF) of X. Hence, the PDF of X can be achieved by using the inverse Fourier transform to the corresponding characteristic function as following

$$f(x) = \frac{1}{2\pi}\int_{-\infty}^{\infty} \Phi_X(\omega) e^{-j\omega x} dx \tag{3.2}$$

Also, there is an important relation between characteristic function and the moments of a random variable: the derivatives of the characteristic function of random variable X are related to its moments. The first derivative of the characteristic function is

$$\frac{d\Phi_X(\omega)}{d\omega} = j\int_{-\infty}^{\infty} x e^{j\omega x} f(x) dx \tag{3.3}$$

By evaluating the derivative at $\omega = 0$, the first moment of random variable X is

$$m_X = -j\frac{d\Phi_X(\omega)}{d\omega}\Big|_{\omega=0} = E(X) \tag{3.4}$$

The nth derivative of $\Phi_X(\omega)$ evaluated at $\omega = 0$ yields the nth moment (this is known as **Moment Theorem**)

$$E(X^n) = (-j)^n \frac{d^n\Phi_X(\omega)}{d\omega^n}\Big|_{\omega=0} = m_X^n \tag{3.5}$$

Moreover, by using characteristic function we are able to easily determine the PDF of a sum of statistically independent random variables. Let X_i, $i = 1, 2, ..., n$, be a set of n statistically independent random variables and

$$Y = \sum_{i=1}^{n} X_i . \tag{3.6}$$

Then we can obtain the characteristic function of random variable Y as

$$\begin{aligned}\Phi_Y(\omega) &= E\left[e^{(j\omega Y)}\right] = E\left[e^{\left(j\omega\sum_{i=1}^{n}X_i\right)}\right] \\ &= E\left[\prod_{i=1}^{n}\left(e^{j\omega X_i}\right)\right] \\ &= \prod_{i=1}^{n}\left[E\left(e^{j\omega X_i}\right)\right] \\ &= \prod_{i=1}^{n}\Phi_{X_i}(\omega)\end{aligned} \tag{3.7}$$

That is the characteristic function of the sum of a set of independent variables is the product of the characteristic functions of the independent variables. Thus the PDF of Y can be determined from the inverse Fourier transform of $\Phi_Y(\omega)$ given by equation 3.7.

Finally, the characteristic function of the convolution of two functions is the product of two characteristic functions relative to the two given functions, which is known as ***Convolution Theorem*** of characteristic function. Let $f_1(x)$ and $f_2(x)$ be two given functions, and $\Phi_1(\omega)$ and $\Phi_2(\omega)$ be the characteristic functions respectively. And also

$$\begin{aligned}f(x) &= f_1(x) * f_2(x) \\ &= \int_{-\infty}^{\infty} f_1(t) f_2(x-t)dt \\ &= \int_{-\infty}^{\infty} f_1(x-t) f_2(x)dt\end{aligned} \tag{3.8}$$

where * means the convolution operation. Then we can obtain the characteristic function $\Phi(\omega)$ of $f(x)$.

$$\Phi(\omega) = \Phi_1(\omega)\Phi_2(\omega) \tag{3.9}$$

In this subsection characteristic function and its some key properties are presented, for further information please refers to (Papoulis 1965; Proakis 2000). Next we will show some useful probability distributions essential to wireless time-varying channel analysis.

3.1.2 Some Useful Probability Distributions

In this subsection some useful probability distributions and their properties are presented. For instance, Exponential distribution, Gaussian (normal) distribution, Chi-square distribution, Non-central Chi-square distribution, Rayleigh distribution, Rice distribution, Nakagami-m distribution, and also the interrelations between them (Jeruchim et al. 2000; Mathword 2008; Papoulis 1965; Proakis 2000).

Gaussian (Normal) Distribution

Probability Density Function:

$$f(x) = \frac{1}{\sigma\sqrt{2\pi}} exp\left[\frac{-(x-\mu_X)^2}{2\sigma^2}\right], \qquad -\infty < x < \infty \tag{3.10}$$

Parameters:

$mean:\ \mu_X$
$variance:\ \sigma^2$

The cumulative distribution function (CDF) is

$$\begin{aligned} F(x) &= \int_{-\infty}^{x} f(r)dr \\ &= \frac{1}{\sigma\sqrt{2\pi}} \int_{-\infty}^{x} exp\left[\frac{-(r-\mu_X)^2}{2\sigma^2}\right] dr \\ &= \frac{1}{2}\frac{2}{\sqrt{\pi}} \int_{-\infty}^{(x-\mu_X)/\sqrt{2}\sigma} e^{-t^2} dt \\ &= \frac{1}{2} + \frac{1}{2} erf\left(\frac{x-\mu_X}{\sqrt{2}\sigma}\right) \end{aligned}, \tag{3.11}$$

Where *erf*(x) means the error function, defined by

$$erf(x) = \frac{2}{\sqrt{\pi}} \int_0^x e^{-t^2} dt \tag{3.12}$$

The CDF and PDF functions are plotted in Fig. 3.1.

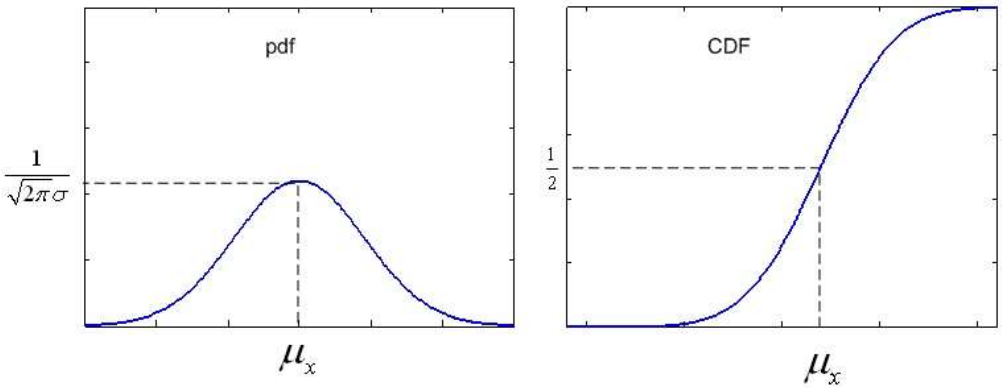

Figure 3.1: The PDF and CDF of Gaussian Distribution.

Exponential Distribution

Probability Density Function:

$$f(x) = \lambda e^{-\lambda x}, \qquad x > 0 \tag{3.13}$$

Parameter:

$$\lambda, \qquad \lambda > 0 \tag{3.14}$$

Mean and Variance:

$$\mu_X = \frac{1}{\lambda}$$
$$\sigma^2 = \frac{1}{\lambda^2} \tag{3.15}$$

The cumulative distribution function (CDF) is

$$F(x) = 1 - e^{-\lambda x}, \qquad x > 0 \tag{3.16}$$

The CDF and PDF functions of exponential distribution are plotted in Fig. 3.2.

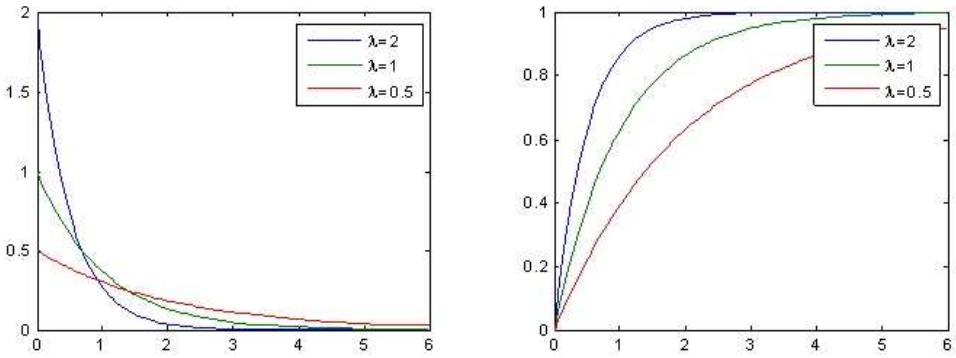

Figure 3.2: The PDF and CDF of Exponential Distribution.

Chi-square Distribution

A chi-square distributed random variable is related to a Gaussian-distributed random variable, that is, when X is a Gaussian random variable with zero mean, $Y = X^2$ follows a chi-square distribution. The PDF is given by

$$f(y) = \frac{1}{\sqrt{2\pi y}\sigma} e^{-y/2\sigma^2}, \qquad y \geq 0 \tag{3.17}$$

The CDF of Y is

$$F(y) = \int_0^y f(u)du = \frac{1}{\sqrt{2\pi}\sigma} \int_0^y \frac{1}{\sqrt{u}} e^{-u/2\sigma^2} du \tag{3.18}$$

which can not be expressed in closed form. The characteristic function is given by

$$\Phi(\omega) = \frac{1}{\sqrt{1 - j2\omega\sigma^2}} \tag{3.19}$$

Next assume that the random variable Y is defined as $Y = \sum_{i=1}^{n} X_i^2$, where X_i, *i=1, 2,..., n,* are statistically independent and identically distributed Gaussian variables with zero mean and variance σ^2. Then according the property proposed in (3.7), the characteristic function of the sum of a set of independent variables is the product of the characteristic functions of the independent variables, we can easily obtain the characteristic function of variable *Y* as

$$\Phi(\omega) = \frac{1}{(1 - j2\omega\sigma^2)^{n/2}} \tag{3.20}$$

Now we can find the PDF of *Y* by inversing the above characteristic function, which yields (Papoulis 1965: 130; Proakis 2000: 45),

$$f(y) = \frac{1}{\sigma^n 2^{n/2} \Gamma(\frac{n}{2})} y^{\frac{n}{2}-1} e^{-\frac{y}{2\sigma^2}}, \qquad y \geq 0 \tag{3.21}$$

where $\Gamma(\cdot)$ is the gamma function. The PDF proposed by equation (3.21) is called a chi-square PDF with n degrees of freedom. The PDF function of chi-square distribution with *n* degrees of freedom is plotted in Figure 3.3.

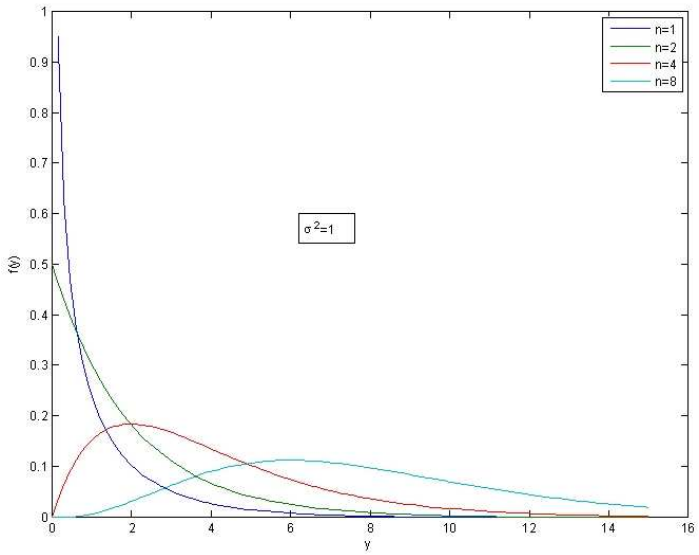

Figure 3.3: The PDF of Chi-square Distribution with *n* Degrees of Freedom.

Non-central Chi-square Distribution

In previous subsection, the central chi-square distribution is discussed briefly where the components X_i are independent Gaussian random variables with zero mean. In this subsection a general case is presented, where X_i are Gaussian random variables with non-zero means. First, the simpler case $Y = X^2$ is considered where *X* has a mean μ and variance σ^2, and then extended to the general situation of $Y = \sum_{i=1}^{n} X_i^2$. For $Y = X^2$, the characteristic function of the random variable Y is given as

$$\Phi(\omega) = \frac{1}{\sqrt{1 - j2\omega\sigma^2}} e^{j\mu^2\omega/(1-j2\omega\sigma^2)} \tag{3.22}$$

In order to generalize the result, let $Y = \sum_{i=1}^{n} X_i^n$, that is Y is the sum of Gaussian random

variables, X_i, i = 1, 2, ..., n, which have statistically independent mean values μ_i, and identical variances equal to σ^2. Then according the property proposed in (3.7), the characteristic function of the sum of a set of independent variables is the product of the characteristic functions of the independent variables, we can easily obtain the characteristic function of variable $Y = \sum_{i=1}^{n} X_i^n$ as

$$\Phi(\omega) = \frac{1}{(1 - j2\omega\sigma^2)^{n/2}} exp\left(\frac{j\omega \sum_{i=1}^{n} \mu_i^2}{(1 - j2\omega\sigma^2)} \right) \tag{3.23}$$

The PDF with *n* degrees of freedom can be received by using inverse Fourier transform to the above characteristic function,

$$f(y) = \frac{1}{2\sigma^2} \left(\frac{y}{\mu^2} \right)^{(n-2)/4} e^{-(\mu^2 + y)/2\sigma^2} I_{n/2-1} \left(\sqrt{y} \frac{\mu}{\sigma^2} \right), \tag{3.24}$$

where

$$\mu^2 = \sum_{i=1}^{n} \mu_i^2 \tag{3.25}$$

is called the non-centrality parameter and $I_k(\cdot)$ is the *k*th-order modified Bessel function of the first kind defined as

$$I_k(z) = \sum_{i=0}^{\infty} \frac{(\frac{z}{2})^{k+2i}}{i!\Gamma(k+i+1)}, \qquad z \geq 0 \tag{3.26}$$

The CDF of non-central chi-square distribution with n degrees of freedom is the integration of PDF as following

$$F(y)=\int_0^y \frac{1}{2\sigma^2}\left(\frac{u}{\mu^2}\right)^{(n-2)/4} e^{-(\mu^2+u)/2\sigma^2} I_{n/2-1}\left(\sqrt{u}\,\frac{\mu}{\sigma^2}\right)du \tag{3.27}$$

From the above equation there is no closed-form expression for this integral. For the case that *n* is even, *n = 2m*, the CDF can be expressed by the generalized Marcum's Q function as

$$\begin{aligned} Q_m(a,b) &= \int_b^a x(\frac{x}{a})^{m-1}\exp(-(\frac{x^2+a^2}{2}))I_{m-1}(ax)dx \\ &= Q_1(a,b)+\exp(-(\frac{x^2+a^2}{2}))\sum_{k-1}^{m-1}(\frac{b}{a})^k I_k(ab) \end{aligned} \tag{3.28}$$

where

$$Q_1(a,b)=\exp(-\frac{x^2+a^2}{2})\sum_0^{\infty}(\frac{b}{a})^k I_k(ab), \qquad b>a>0 \tag{3.29}$$

Then the CDF of variable Y comes to

$$F(y)=1-Q_m(\frac{\mu}{\sigma},\frac{\sqrt{y}}{\sigma}) \tag{3.30}$$

The CDF and PDF functions of non-central chi-square distribution are plotted in Fig. 3.4.

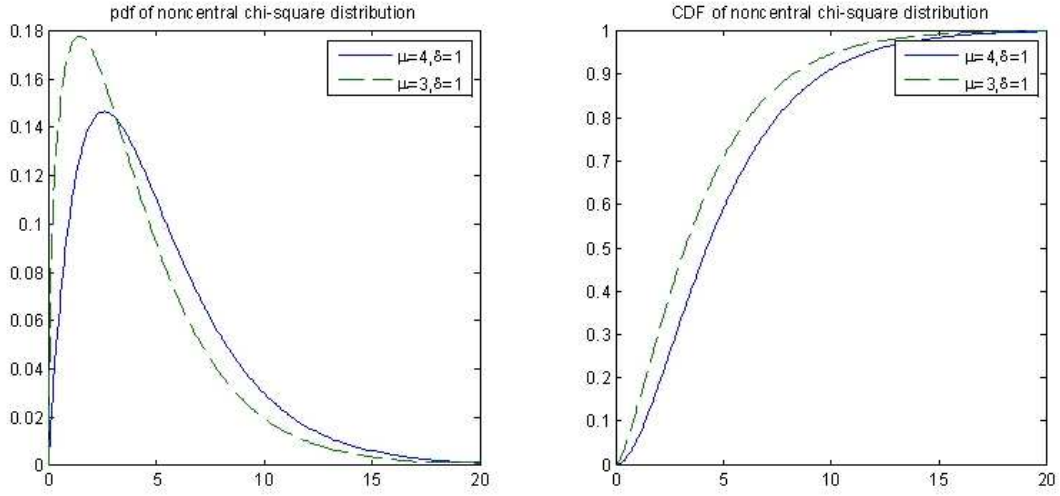

Figure 3.4: The PDF and CDF of Non-central Chi-Square Distribution.

Rayleigh Distribution

Rayleigth distribution has various applications in wireless communications, such as statistic signals analysis in wireless communication channels. Next we will introduce the characteristics of this key distribution. Let X_1, X_2 be zero-mean independent Gaussian random variables with a variance σ^2, and $Y = \sqrt{X_1^2 + X_2^2}$. We know that Y^2 follows chi-square distribution which is presented previously. However, Y is a Rayleigh-distributed random variable. The probability density function (PDF) is given as

$$f(y) = \frac{y}{\sigma^2} e^{-y^2/2\sigma^2}, \qquad y \geq 0 \tag{3.31}$$

The corresponding cumulative distribution function (CDF) is

$$F(y) = 1 - e^{-y^2/2\sigma^2}, \qquad y \geq 0 \tag{3.32}$$

The CDF and PDF functions of Rayleigth distribution are plotted in Fig. 3.5.

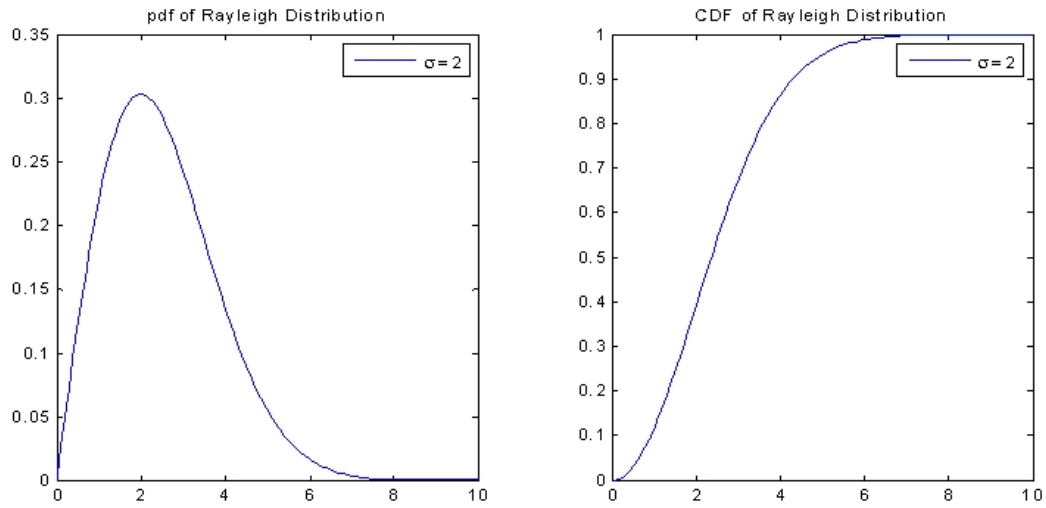

Figure 3.5: The PDF and CDF of Rayleigth Distribution.

Rice Distribution

In the previous subsection we present that the variable $Y = \sqrt{X_1^2 + X_2^2}$ is a Rayleigh-distributed random variable when X_1 and X_2 are zero mean Gaussian random variables. In this part another case is introduced that $Y = \sqrt{X_1^2 + X_2^2}$, where X_1 and X_2 are non-zero mean Gaussian random variables with means μ_i, i = 1, 2 and variance σ^2. Under this situation the random variable *Y* has a Rician distribution, and the PDF is given as following,

$$f(y) = \frac{y}{\sigma^2} e^{-(y^2+\mu^2)/2\sigma^2} I_0(\frac{y\mu}{\sigma^2}), \qquad y \geq 0 \tag{3.33}$$

where $\mu^2 = \mu_1^2 + \mu_2^2$, and I_0 is the zero-order modified Bessel function of the first kind. The CDF of Y is given by

$$F(y) = 1 - Q_1(\frac{\mu}{\sigma}, \frac{y}{\sigma}), \qquad y \geq 0 \tag{3.34}$$

where $Q_1(a,b)$ is defined by equation 3.28. The CDF and PDF functions of Rice distribution are plotted in Fig. 3.6.

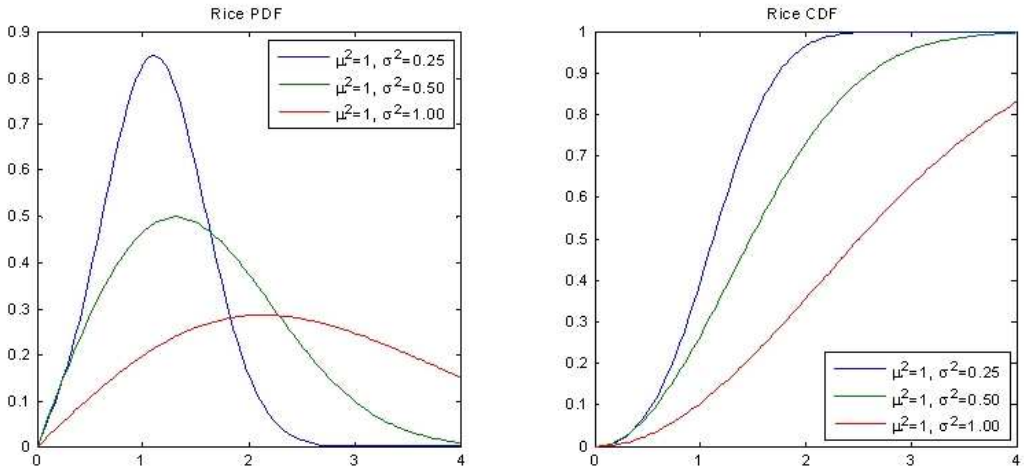

Figure 3.6: The PDF and CDF of Rice Distribution.

Nakagami-m Distribution

As we know that Rayleigh distribution and Rice distribution are frequently utilized to analyze the statistical signal characteristics which are quite important to design the wireless systems (Goldsmith 2005; Parsons 1999; Proakis 2000; Rappaport 2002; Sklar 2001). Also another distribution is used to characterize the random signals through multipath fading channels is Nakagami m-distribution (Nakagami 1960). The PDF for Nakagami-m distribution is given by Nakagami as

$$f(y) = \frac{2}{\Gamma(m)}\left(\frac{m}{\Omega}\right)^m y^{2m-1} e^{-my^2/\Omega} \tag{3.35}$$

where $\Gamma(\cdot)$ is the gamma function, m and Ω are parameters of Nakagami-m distribution, which $\Omega = E(Y^2)$ is the second moment and m is the ratio of moments, known as the *fading figure* defined as

$$m = \frac{\Omega^2}{E\left[(Y^2 - \Omega)^2\right]}, \qquad m \geq 0.5 \tag{3.36}$$

By letting $m = 0.5$ we can find that the equation 3.35 reduces to the one-side Gaussian distribution, and for $m = 1$ it becomes Rayleigh distribution by comparing to the equation 3.31. For the values of m in the range $0.5 \leq m \leq 1$, from Fig. 3.7 we can find that PDFs have larger tails than a Rayleigh-distributed random variable, but for m>1, the tails decay faster.

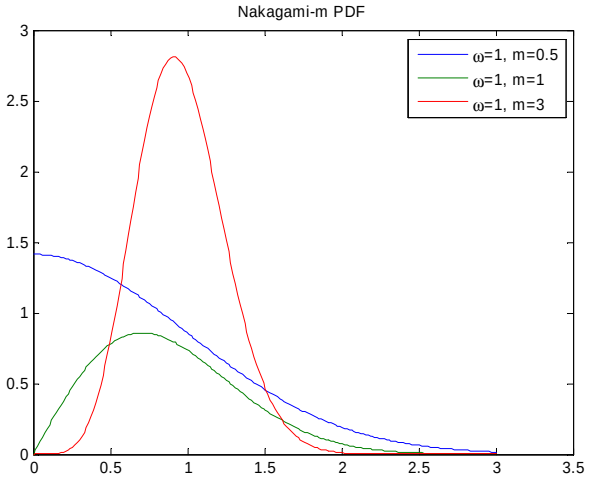

Figure 3.7: The PDF of Nakagami-m Distribution.

Lognormal Distribution

Assume that a random variable *X* is normally distributed with mean μ and variance σ^2. Then the new variable *Y*, where $Y = e^X$ or $X = \ln(Y)$ is a log-normally distributed random variable. Its PDF is given as

$$f(y) = \begin{cases} \dfrac{1}{y\sqrt{2\pi}\sigma} e^{-(ln(y)-\mu)^2/2\sigma^2}, & y \geq 0 \\ 0, & y \leq 0 \end{cases} \tag{3.37}$$

And the CDF is

$$F(y) = \frac{1}{2} + \frac{1}{2} erf\left[\frac{ln(y)-\mu}{\sigma\sqrt{2}}\right], \qquad y \geq 0 \tag{3.38}$$

where μ and σ are the mean and standard deviation of the normally distributed random variable *X*. The CDF and PDF functions of Lognormal distribution are plotted in Fig. 3.8.

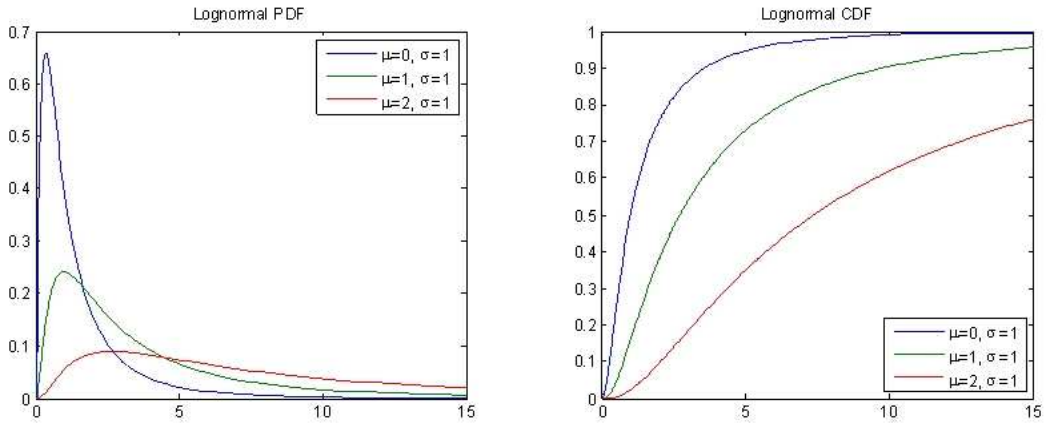

Figure 3.8: The PDF and CDF of Lognormal Distribution.

Summary to the Various Distributions

In this subsection, we summarize the distributions mentioned above by providing the main interrelations between different distributions.

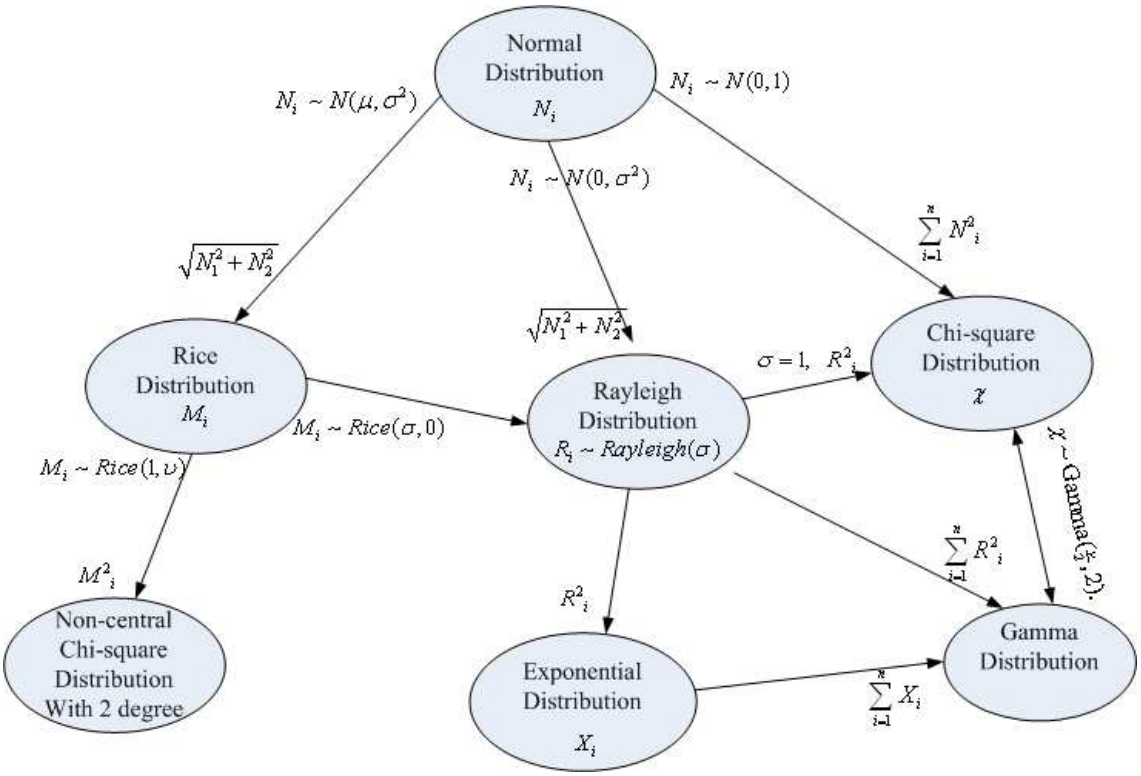

Figure 3.9: Interrelations Between Different Distributions.

3.1.3 Autocorrelation, Cross correlation, and Power Spectral Density

Correlation functions are used to analyze the statistical parameters of linear systems (Lee 1982). If the two random variables are from the same random process, the correlation methodology will be autocorrelation, and if they are from different random

processes, it will be cross correlation. The power spectral density (PSD) of a random process is the Fourier transform of the autocorrelation function.

Autocorrelation

Let assume a complex-valued random process:

$$Z(t) = X(t) + jY(t) \tag{3.39}$$

where *X(t)* and *Y(t)* are real random processes. The autocorrelation function of *Z(t)* is

$$\begin{aligned} R_{ZZ}(t_1,t_2) &= \frac{1}{2}E\left[Z(t_1)Z^*(t_2)\right] \\ &= \frac{1}{2}E\left[(X(t_1)+jY(t_1))(X(t_2)-jY(t_2)\right] \\ &= \frac{1}{2}E\left[X(t_1)X(t_2)+Y(t_1)Y(t_2)+jY(t_1)X(t_2)-jX(t_1)Y(t_2)\right] \\ &= \frac{1}{2}\left[R_{XX}(t_1,t_2)+R_{YY}(t_1,t_2)\right]+j\frac{1}{2}\left[R_{YX}(t_1,t_2)-R_{XY}(t_1,t_2)\right] \end{aligned} \tag{3.40}$$

For a wide-sense stationary random process, which correlation function only depends on the time difference $\tau = t_2 - t_1$, the autocorrelation becomes $R_{ZZ}(\tau) = R_{ZZ}(t_1,t_2)$, and the equation (3.40) comes to

$$R_{ZZ}(\tau) = \frac{1}{2}\left[R_{XX}(\tau)+R_{YY}(\tau)\right]+j\frac{1}{2}\left[R_{YX}(\tau)-R_{XY}(\tau)\right] \tag{3.41}$$

Cross Correlation

Let assume two complex-valued random processes:

$$Z(t) = X(t) + jY(t)$$
$$U(t) = H(t) + jG(t)$$

where *X(t), Y (t), H(t),* and *G(t)* are real random processes. The cross correlation of *Z (t)* and *U(t)* is

$$\begin{aligned} R_{ZU}(t_1,t_2) &= \frac{1}{2}E\left[Z(t_1)U^*(t_2)\right] \\ &= \frac{1}{2}E\left[(X(t_1)+jY(t_1))(H(t_2)-jG(t_2)\right] \\ &= \frac{1}{2}E\left[X(t_1)H(t_2)+Y(t_1)G(t_2)+jY(t_1)H(t_2)-jX(t_1)G(t_2)\right] \\ &= \frac{1}{2}\left[R_{XH}(t_1,t_2)+R_{YG}(t_1,t_2)\right]+j\frac{1}{2}\left[R_{YH}(t_1,t_2)-R_{XG}(t_1,t_2)\right]. \end{aligned} \tag{3.42}$$

For two wide-sense stationary random processes, which correlation function only depends on the time difference $\tau = t_2 - t_1$, the cross correlation becomes $R_{ZU}(\tau) = R_{ZU}(t_1,t_2)$, and the equation (3.42) comes to

$$R_{ZU}(\tau) = \frac{1}{2}\left[R_{XH}(\tau)+R_{YG}(\tau)\right]+j\frac{1}{2}\left[R_{YH}(\tau)-R_{XG}(\tau)\right] \tag{3.43}$$

Power Spectral Density

The power spectral density (PSD), $\Psi_{XX}(f)$, and the relative autocorrelation function, $R_{XX}(\tau)$, of a random process $X(t)$ are a Fourier transform pair,

$$\begin{aligned} \Psi_{XX}(f) &= \int_{-\infty}^{\infty} R_{XX}(\tau)e^{-j2\pi f\tau}d\tau \\ R_{XX}(\tau) &= \int_{-\infty}^{\infty} \Psi_{XX}(f)e^{j2\pi f\tau}df \end{aligned} \tag{3.44}$$

The Parseval's theorem gives the way by using the correlation function to calculate the power P in a random process *X(t)* as

$$\begin{aligned} P &= E\left[X^2(t)\right] \\ &= R_{XX}(0) \\ &= \int_{-\infty}^{\infty} \Psi_{XX}(f)df. \end{aligned} \tag{3.45}$$

For the case of two random process *X(t)* and *Y (t),* the cross power spectral density is

$$\Psi_{XY}(f) = \int_{-\infty}^{\infty} R_{XY}(\tau)e^{-j2\pi f\tau}d\tau \tag{3.46}$$

3.2. Small-Scale Multipath Propagation Characteristics

Small-scale fading describes the rapid variations of the amplitudes, phase, or multipath delays of a radio signal over a short period of time or travel distance. The fading is due to the time differences among the arrived signals at the receiver, which are called multipath waves. Thus the combined received signal varies randomly and rapidly in amplitude and phase.

3.2.1 Factors Influencing Small-Scale Fading

There are a lot of physical factors influencing the small-scale fading in the radio channel, such as (Rappaport 2002: 177-179):

- Multipath propagation
  - Rapid changes in signal strength over a small travel distance or time interval.

- Random frequency modulation due to varying Doppler shifts on different multipath signals.
- Time dispersion caused by multipath propagation delays.

• Speed of the mobile

- The relative motion between the mobile and the base station results in different Doppler shifts on each of the multipath, which depend on the carrier frequency, moving speed, and the arrival direction of the signal.
- And also moving direction, which decides the sign of Doppler shift, positive or negative. If the mobile moves toward the base station, it will be positive, otherwise negative.

• Speed of surrounding objects

- Not only the motion of mobile terminals effect the Doppler shifts, but the moving objects in the radio channel cause time-varying Doppler shifts on multipath components. If the surrounding objects move at a greater rate than the mobile, then this effect dominates the small-scale fading. Otherwise, it can be ignored, and only the speed of the moving mobile need to be considered.

• The transmission bandwidth of the signal

- If the transmitted radio signal bandwidth is larger than the coherence bandwidth of the multipath channel, the received signal will be distorted, but the small scale fading will not be significant that the received signal strength will not fade much over local area.
- If the transmitted signal has a narrow bandwidth compared to the channel, the received signal will vary rapidly, but the signal will not be distorted in time.

3.2.2 Doppler Shift

As we have discussed in previous subsection that the mobility of the mobile will cause some fading in received signal strength. Thus in order to explain this phenomenon we use the concept of Doppler shift. As we know that there exist some time differences among the waves traveling different path lengths between the transmitter and the receiver, which cause the phase change in the received signal. In consequence, the apparent changes also occur in frequency, known as Doppler shift. Next we will illustrate it by using a simple example.

Example: The receiver is moving at a speed of v along a path with distance *d*, and the antenna receives signals from the transmitter (Fig. 3.9). And also assume that the distance from the transmitter to the receiver is much larger that *d*, so we can have the arrival angles of two received signal are approximately equal.

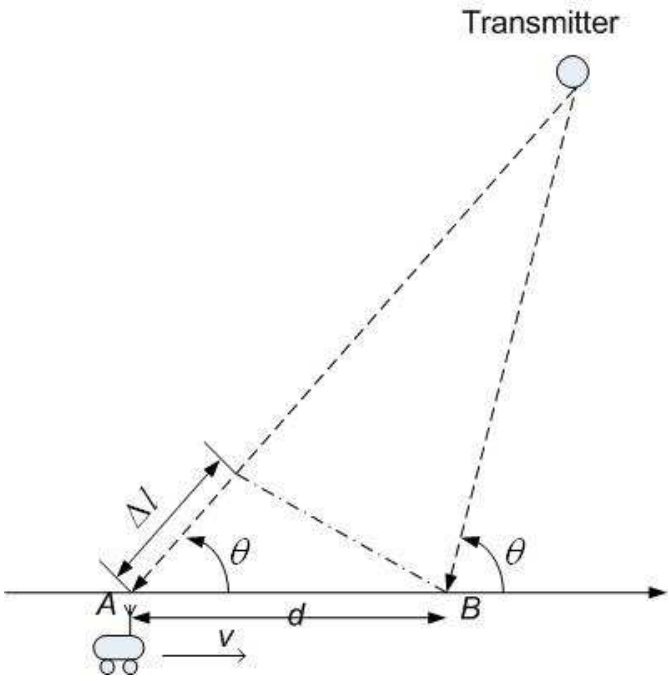

Figure 3.10: Illustration of a Direct Path and a Reflected one.

Answer: The path length differences between the two received signals propagation is $\Delta l \approx d\cos\theta = v\Delta t\cos\theta$, where Δt is the time that the mobile moves from point A to B. Then we can obtain the phase difference between the two received signals due to different propagation path length as

$$\Delta\phi = \frac{2\pi\Delta l}{\lambda}\cos\theta, \tag{3.47}$$

where λ is the wave length of the transmitted signal. Therefore the frequency change, or Doppler Shift, is

$$f_d = \frac{\Delta\phi}{2\pi\Delta t} = \frac{v}{\lambda}\cos\theta \tag{3.48}$$

From this simple example, we can find that the Doppler shift is related to the moving speed and direction of the mobile. If the mobile is moving toward the direction of radio wave arriving, the Doppler shift is positive. Otherwise, it is negative.

3.3 Several Important Parameters of Multipath Channels

3.3.1 Time Dispersion Parameters

Mean Excess Delay

The mean excess delay is defined as the first moment of the power delay profile (Rappaport 2002: 197-200),

$$\overline{\tau} = \frac{\sum_k P(\tau_k)\tau_k}{\sum_k P(\tau_k)} \tag{3.49}$$

where $P(\tau_k)$ is the received power of delayed *k*th path, and τ_k is the *k*th path delay.

RMS Delay Spread

The RMS (root mean square) delay spread is the square root of the second central moment of the power delay profile (Rappaport 2002: 197-200), given by

$$\delta_\tau = \sqrt{\overline{\tau^2} - (\overline{\tau})^2} \tag{3.50}$$

where

$$\overline{\tau^2} = \frac{\sum_k P(\tau_k)\tau_k^2}{\sum_k P(\tau_k)} \tag{3.51}$$

and $P(\tau_k)$ is the received power of delayed *k*th path, and τ_k is the *k*th path delay.

Example:

This simple example shows how to use the above to compute the mean excess delay and rms delay spread. The power delay profile and path delays are given in following Fig. 3.10.

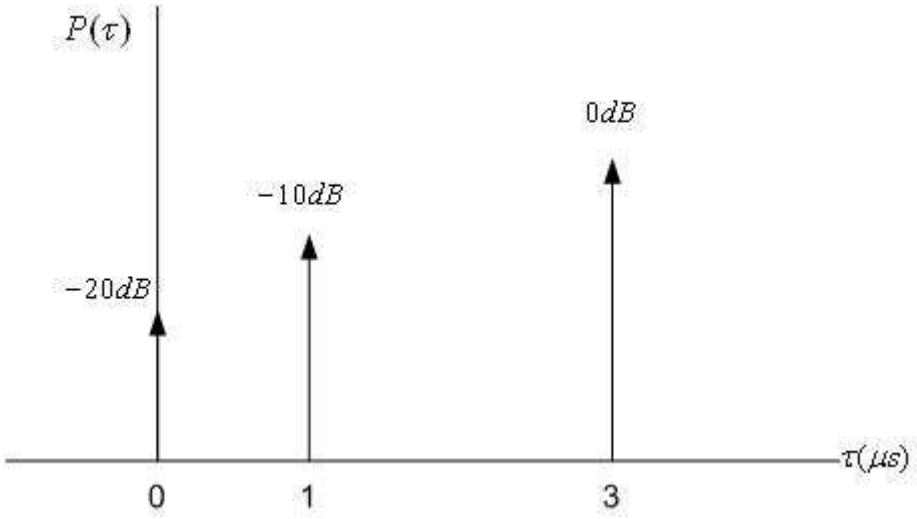

Figure 3.11: Example: RMS Delay Spread.

Solution:

$$\overline{\tau} = \frac{10^{-0.2}\times 0 + 10^{-0.1}\times 1 + 10^{0}\times 3}{10^{-0.2}+10^{-0.1}+10^{0}} = 1.5645\mu s$$

$$\overline{\tau^2} = \frac{10^{-0.2}\times 0^2 + 10^{-0.1}\times 1^2 + 10^{0}\times 3^2}{10^{-0.2}+10^{-0.1}+10^{0}} = 4.0384\mu s$$

$$\delta_\tau = \sqrt{\overline{\tau^2} - (\overline{\tau})^2} = \sqrt{4.0384 - 1.5645^2} = 1.2613\mu s$$

3.3.2 Coherence Bandwidth

According to (Lee 1982: 130), the different time delays in two fading signals that are closely spaced in frequency can cause the two signals to become correlated. Coherence bandwidth is a measure of the range of frequency spacing over which the channel can be considered as flat which means that all spectral components undergo approximately equal gain and linear phase. If the coherence bandwidth is defined as the bandwidth

over which the frequency correlation function is above 0.9, then the coherence bandwidth is approximately (Lee 1982: 133-150; Rappaport 2002: 202)

$$B_c \approx \frac{1}{50\delta_\tau}, \tag{3.52}$$

and if the frequency correlation function is above 0.5, then the coherence bandwidth is approximately

$$B_c \approx \frac{1}{5\delta_\tau}, \tag{3.53}$$

where δ_τ is the rms delay.

3.3.3 Doppler Spread

Doppler spread D_s describes the time-varying characteristics of a channel, which is cause by the relative mobility between the transmitter and the receiver or also the movement of the objects in the channel. Doppler spread is defined as the range of the frequencies over which the received Doppler spectrum is essentially non-zero (Rappaport 2002: 203). Thus it is the measure of the spectral spreading caused by the time rate of mobile channel variation. The Doppler spectrum is defined as the received signal spectrum when the transmitted signal is a pure sinusoidal signal with frequency f_c, and the range is from $f_c - f_D$ to $f_c + f_D$, where f_D is the Doppler shift.

3.3.4 Coherence Time

Besides Doppler Spread, Coherence Time T_c is another parameter describing the time-varying characteristics of a channel. From (Rappaport 2002: 198-205), coherence time is the time domain dual of Doppler spread and is used to characterize the time-varying

nature of the frequency dispersion of the channel in time domain. During the coherence time, the channel impulse response can be considered to be invariant. The coherence time and Doppler spread are inversely proportional to another (Rappaport 2002: 203),

$$T_c \approx \frac{1}{f_m} , \tag{3.53}$$

where $f_m = v / \lambda$ is the maximum Doppler shift.

3.4 Types of Small-Scale Fading

As what we showed in Fig. 3.2 the fading types experienced by a signal via a radio channel are characterized by the transmitted signal and also the characteristics of the channel. And we also illustrate in previous sections that the relation between the transmitted signal parameters, for example bandwidth, and the channel parameters, for instance RMS delay spread and Doppler spread, will affect the transmitted signal undergoing different types of fading. The time dispersion and frequency dispersion mechanisms in mobile radio channels lead to four possible distinct effects, that is, multipath delay spread leads to time dispersion and frequency selective fading, while Doppler spread leads to frequency dispersion and time selective fading (Rappaport 2002: 205-210; Sklar 2001: 947-970). In Tables 3.1 and 3.2, we show a simplified tree of the four different types of fading, which comes from the Fig 2.2.

Table 3.1: Small-Scale Fading Based on Time Spreading

Flat Fading (Frequency Non-Selective Fading)	**Frequency Selective Fading**
1. Signal bandwidth < Channel bandwidth	1. Signal bandwidth > Channel bandwidth
2. Delay spread < Symbol period	2. Delay spread > Symbol period

Table 3.2: Small-Scale Fading Based on Doppler Spread

Fast Fading	**Slow Fading**
1. High Doppler Spread	1. Low Doppler Spread
2. Coherence time < Symbol period	2. Coherence time > Symbol period
3. Channel variations are faster than baseband signal variations	3. Channel variations are slower than baseband signal variations

3.4.1 Small-Scale Fading Based on Time Spreading

Time dispersion due to multipath causes the transmitted signal to undergo either flat (frequency non-selective) or frequency selective fading (Rappaport 2002: 205-210; Sklar 2001: 947-970). The fading channel manifestations are illustrated in Fig. 2.2.

Flat Fading

A channel is considered as flat fading, or frequency non-selective fading, if the maximum excess delay time is less than the symbol duration, which means that all

multipath components of a transmitted symbol arrive within the symbol duration. Therefore the components are not resolvable (Rappaport 2002: 205). Although there is no channel-induced inter symbol interference (ISI), the SINR will be degraded by adding up the irresolvable components destructively, and the signal also can sometimes experience the distortion effects of frequency selective fading. We use Fig. 3.12 to illustrate the characteristics of a flat fading channel.

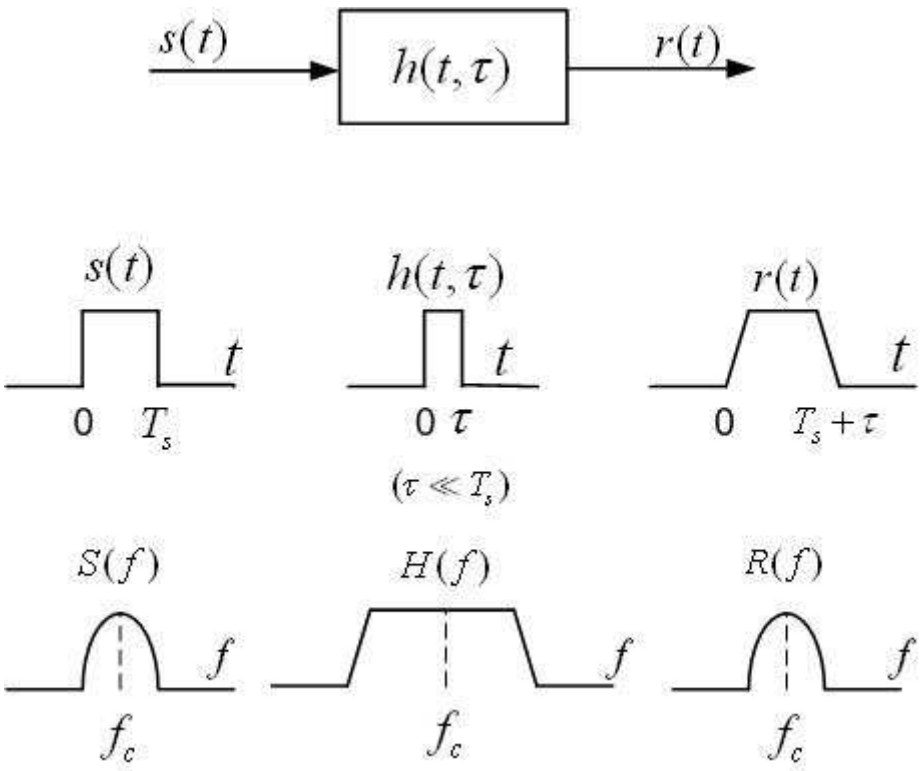

Figure 3.12: Flat Fading Channel Characteristics (Rappaport 2002: 207).

From Fig. 3.12, we can find that if the channel gain changes over time, the received signal amplitude also changes, while the transmitted signal spectrum is preserved.

Frequency Selective Fading

A channel is considered as frequency selective fading, if the maximum excess delay time is larger than the symbol duration which means that the channel impulse response has a multipath delay spread. In this case the many multipath components are resolvable by the receiver. In addition, the received signal is distorted due to faded and delayed multipath components, which are inter-symbol interference. Fig. 3.13 illustrates the characteristics of frequency selective fading.

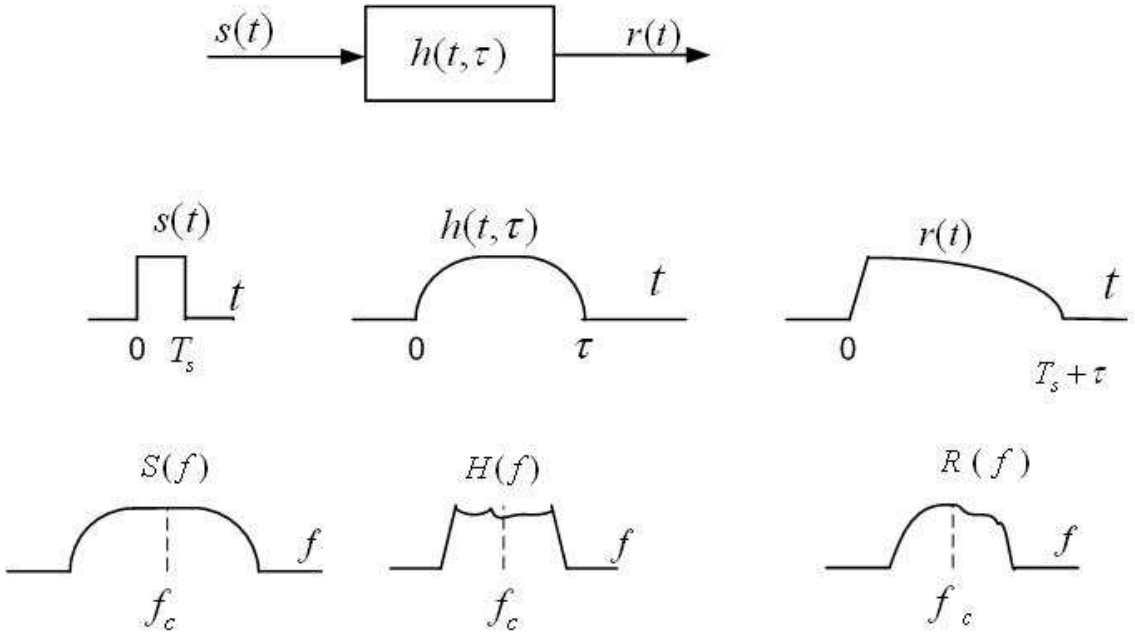

Figure 3.13: Frequency Selective Fading Channel Characteristics (Rappaport 2002: 208).

From Fig. 3.12, we can find that for the frequency selective fading the transmitted signal spectrum has a larger bandwidth than the channel coherence bandwidth. Also, different frequency components have different channel gains.

3.4.2 Small-Scale Fading Based on Time Variation

Previously, we discussed the small-scale fading, where signal dispersion and coherence bandwidth characterize the time spreading but not provide the information on channel time-varying aspects. In this subsection we will introduce another small-scale fading due to time variation characteristics of radio channels. Based on how rapidly the transmitted baseband signal changes compared to the rate of channel changing, a channel may be classified either as a fast fading or slow fading channel (Rappaport 2002: 208).

Fast Fading

In fast fading channel, the coherence time of the channel is smaller than the symbol duration, where the channel changes fast rapidly within the symbol duration. Therefore, a signal will undergo fast fading if $T_s > T_c$ or $B_s < B_D$, where T_s is the symbol duration, T_c is the channel coherence time, B_D is the Doppler spread, and B_s is the baseband signal bandwidth. Fig. 3.13 illustrates the envelope with Rayleigh distribution of a faded signal.

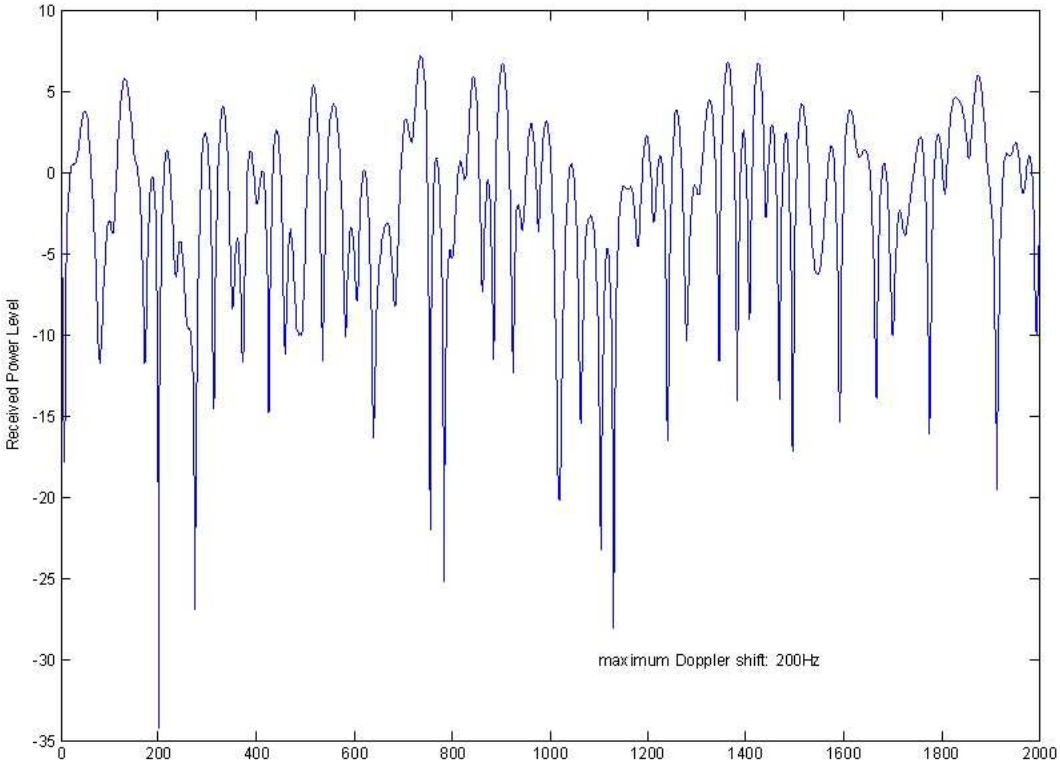

Figure 3.14: A Faded Signal envelope with Rayleigh distribution

Slow Fading

In a slow fading channel, the channel impulse response changes much slower than the transmitted baseband signal does. This means that the Doppler spread of the channel is much less than the baseband signal bandwidth, $T_s << T_c$ or $B_s >> B_D$. Here are some concepts must be taken seriously in order to catch flat fading, frequency selective fading, fast fading, and slow fading:

- The multipath delay spreading determines whether a signal undergoes flat fading or frequency selective fading.

• The time variation or Doppler spread, which is depends on the motion of the mobile or objects in the channel, determines whether a signal undergoes fast fading or slow fading.

• It does not mean that a channel can not be flat or frequency selective fading while undergoing fast or slow fading.

3.5 Statistical Multipath Channel Models

In this subsection, we will introduce a crucial channel model, multipath channel. In a typical urban environment, a radio signal transmitted from a fixed source to a mobile receiver experiences extreme variation in both amplitude and phase. This variation is due to multipath, which arises when the transmitted signal is reflected, diffracted, or scattered by an object, as that illustrated in Figure 3.14. We can notice the variations of the superposition signal envelope at the receiver. The additional copies of the transmitted signal can be attenuated in power, delayed in time, and shifted in phase and/or frequency from the LoS signal. As a consequence of Multipath affects, the amplitude of the received combined signal can vary constructively or destructively and the time delay of each path causes inter-symbol interference if the signal bandwidth is larger than the inverse of the delay spread (Goldsmith 2005). In a static environment where the transmitter, receiver, and reflectors are all static, the constructive and destructive interference of the multiple paths, and their delays relative to the LoS path, are fixed. However, if the transmitter or receiver, even the obstacles in the vicinity along with the transmission paths are moving, then the characteristics of multiple paths vary with time. These time variations are deterministic when the number, location, and characteristics of the reflectors are known, otherwise, statistical models must be considered (Goldsmith 1994).

3.5.1 Time-Varying Channel Impulse Response

Let us model the transmitted signal as (Goldsmith 2005: 45),

$$\begin{aligned} s(t) &= \Re\left\{u(t)e^{j2\pi f_c t}\right\} \\ &= \Re\{u(t)\}cos(2\pi f_c t) - \Im\{u(t)\}sin(2\pi f_c t) \\ &= x(t)cos(2\pi f_c t) - y(t)sin(2\pi f_c t) \end{aligned} \tag{3.54}$$

where $u(t) = x(t) + jy(t)$ is a complex baseband signal or complex envelope, and $x(t) = \Re\{u(t)\}$, $Y = \Im\{u(t)\}$ are the in-phase and quadrature component respectively. The frequency of $u(t)$ is f_c, which has a bandwidth of B_u. Thus the relative received signal which is the superposition of all *N* path components between the transmitter and the receiver including the line-of-sight (LoS) path and all resolvable multipath ones. In consequence, it comes to

$$r(t) = \Re\left\{\sum_{k=0}^{N} \alpha_k(t)u(t-\tau_k(t))e^{j\left[2\pi f_c(t-\tau_k(t))+\phi_{D_k}\right]}\right\} \tag{3.55}$$

where $n = 0$ represents the LoS path, τ_k is the propagating delay corresponding to path *k* which is given by $d_k(t)/c$, the propagating path length divided by the speed of light, ϕ_{D_k} is the Doppler shift relative to path *k*, and $\alpha_k(t)$ is amplitude, a function of path loss and shadowing. Then the equation 3.55 can be simplified by letting $\phi_k(t) = 2\pi f_c \tau_k(t) - \phi_{D_k}$ to

$$r(t) = \Re\left\{\left[\sum_{k=0}^{N} \alpha_k(t)e^{-j\phi_k(t)}u(t-\tau_k(t))\right]e^{j2\pi f_c t}\right\}. \tag{3.56}$$

As we know that the received signal $r(t)$ is the convolution between the baseband input signal $u(t)$ and the equivalent lowpass time-varying channel impulse response $h(t)$, and then modulated with carrier frequency f_c. Thus we also can express $r(t)$ as

$$r(t) = \Re\left\{\left(\int_{-\infty}^{\infty} h(t)u(t-\tau)d\tau\right)e^{j2\pi f_c t}\right\}. \tag{3.57}$$

From comparing the equation 3.56 and 3.57, we can find the time-varying channel impulse response $h(t)$ is

$$h(t) = \sum_{k=0}^{N} \alpha_k(t)e^{-j\phi_k(t)}\delta(\tau - \tau_k(t)). \tag{3.58}$$

We can verify the equation 3.58 as following,

$$\begin{aligned}
r(t) &= \Re\left\{\left[\int_{-\infty}^{\infty} h(t)u(t-\tau)d\tau\right]e^{j2\pi f_c t}\right\} \\
&= \Re\left\{\left[\int_{-\infty}^{\infty} \sum_{k=0}^{N} \alpha_k(t)e^{-j\phi_k(t)}\delta(\tau-\tau_k(t))u(t-\tau)d\tau\right]e^{j2\pi f_c t}\right\} \\
&= \Re\left\{\left[\sum_{k=0}^{N} \alpha_k(t)e^{-j\phi_k(t)}\left(\int_{-\infty}^{\infty}\delta(\tau-\tau_k(t))u(t-\tau)d\tau\right)\right]e^{j2\pi f_c t}\right\} \\
&= \Re\left\{\left[\sum_{k=0}^{N} \alpha_k(t)e^{-j\phi_k(t)}u(t-\tau_k(t))\right]e^{j2\pi f_c t}\right\}
\end{aligned}$$

3.5.2 Received Signal Envelope and Power Distributions

Rayleigh Fading Channel

As we have illustrated in section 3.1 that for any two Gaussian random variables X_1 and X_2 with zero mean and variance σ^2, then the new variable $Y = \sqrt{X_1^2 + X_2^2}$ is Rayleigh-distributed and Y^2 is exponentially distributed. Let assume that r_I and r_Q are the in-phase and the quadrature components of the received signal at the receiver respectively, which are zero-mean Gaussian random variables with variance σ^2. Then the received signal envelope $R(t) = |r(t)| = \sqrt{r_I^2(t) + r_Q^2(t)}$ is Rayleigh-distributed with the PDF of

$$f_R(r) = \frac{r}{\sigma^2} e^{-r^2/2\sigma^2}, \qquad r \geq 0 \tag{3.59}$$

The power of received signal, $P_r = R^2(t) = r_I^2(t) + r_Q^2(t)$, follows exponential distribution with the following PDF

$$p_r(p) = \frac{1}{2\sigma^2} e^{-p/2\sigma^2}, \qquad r \geq 0 \tag{3.60}$$

Rician Fading Channel

If there is a LoS component existing in the case that we discussed in Rayleigh fading channel section, the channel will follow Rician distribution. Now $r_I(t)$ and $r_Q(t)$ are uncorrelated Gaussian random processes with non-zero means $\mu_I(t)$ and $\mu_Q(t)$

respectively, and the same variance σ^2. Thus the PDF of the received complex signal envelope is

$$f(r) = \frac{r}{\sigma^2} e^{-(r^2+\mu^2)/2\sigma^2} I_0(\frac{r\mu}{\sigma^2}), \qquad r \geq 0 \tag{3.61}$$

where $\mu^2 = \mu_1^2 + \mu_2^2$ is the non-central parameter, and I_0 is the zero-order modified Bessel function of the first kind. Next we introduce another important parameter, Rice Factor *K*, which is the ratio of the dominant power μ_2 to the multipath power $2\sigma^2$, $K = \frac{\mu^2}{2\sigma^2}$. Thus we can obtain a Rayleigh fading if the Rice factor *K = 0*, which means that the Rayleigh fading is a special case of Rician fading. Then the equation (3.61) becomes

$$f(r) = \frac{2r(K+1)}{\Omega_p} exp\left\{-K - \frac{(K+1)r^2}{\Omega_p}\right\} I_0\left(2r\sqrt{\frac{K(K+1)}{\Omega_p}}\right), \qquad r \geq 0 \tag{3.62}$$

where $\Omega_p = \mu^2 + 2\sigma^2$ is the average envelope power. Therefore the power of received signal, $P_r = R^2(t) = r_I^2(t) + r_Q^2(t)$, follows non-central chi-square distribution with the following PDF

$$p_r(p) = \frac{(K+1)}{\Omega_p} exp\left\{-K - \frac{(K+1)p}{\Omega_p}\right\} I_0\left(2\sqrt{\frac{K(K+1)p}{\Omega_p}}\right), \qquad p \geq 0 \tag{3.63}$$

Nakagami Fading Channel

The Nakagami distribution was selected to fit empirical data, and is known to provide a closer match to some experimental data than Rayleigh, Ricean, or lognormal

distributions (Charash 1979; Nakagami 1960). When the Nakagami fading factor $m=1$, the Nakagami fading becomes a Rayleigh distribution; when $m=0.5$, it becomes a one-sided Gaussian fading; when $m\to\infty$, it becomes an impulse which means there no fading any more; last, let Rician factor $K=\frac{\sqrt{m^2-m}}{m-\sqrt{m^2-m}}$ or $m=\frac{(K+1)^2}{2K+1}$, the Nakagami fading can be used to approximate Rician fading. For Nakakami fading channel the PDF of the received signal envelope is

$$f(r)=\frac{2}{\Gamma(m)}\left(\frac{m}{\Omega}\right)^m r^{2m-1}e^{-mr^2/\Omega} \tag{3.64}$$

where parameters m and Ω are given in section (3.1). The power of received signal follows Gamma distribution given by

$$p_r(p)=\left(\frac{m}{\Omega}\right)^m \frac{p^{m-1}}{\Gamma(m)}exp\left(-\frac{mp}{\Omega}\right) \tag{3.65}$$

4. INTRODUCTION TO RADIO RESOURCE MANAGEMENT

In the past decade, the wireless communication technologies have achieved great development. However, the rapid increase of the population of the wireless mobile users and also their demands for obtaining high data rate, high quality of services produce challenging requirements to current wireless communications, especially on the limited spectrum resource allocation. To manage the limited spectral resource is of critical importance to cope with the increasing of users' demands. Thus various algorithms have been developed to optimize the radio resource in order to obtain the required Quality Of Service (QoS) for users. In this chapter, some essential information and techniques on optimizing radio resource are presented. First the main tasks of radio resource management are stated. Second, the power control schemes are presented which are the main contents in this thesis. Then we use power control schemes to cope with the problems raised in bad channel conditions. The objective of the Radio Resource Management scheme is to maximize the system capacity, increase the reliability of the wireless system, and improve the service quality, and so on. The radio resource management algorithm contains the following main tasks (there are also others which are also important, such as handoff, channel allocation, etc.):

- **Power Control**

  Power Control is used to balance the received SINR in order to establish the communication link or match the target SINR. There are many factors in power control should be considered, for instance, wireless channel variation, power control time delay, the interferences to other devices, the lifetime of the battery of mobile terminals, and so on. We will discuss power control in detail later.

- **Rate Control**

Many present wireless system now support multirate data transmission, for instance in CDMA systems, BPSK, QPSK, 16QAM, and etc. modulation schemes are supported. Thus the data rate can be adapted by adjusting the processing gain, which is the proportion of chip rate and bit rate. However, increasing the data rate will increase the bit error rate probability or block error probability (Sklar 2001).

- **Admission Control**

Admission control (AC) is one of the key tasks in radio resource management. It is utilized to accept or reject the new service requests, and also the requests asked by ongoing services in order to obtain higher network resources. In addition, AC is a guarantee of minimizing the probability of the network getting congested.

- **Time Scheduling**

In the time scheduling scheme, transmissions of mobiles are scheduled in time. Each mobile reports its status to the base station (BS) through the reverse request channel (R-REQCH), which conveys the information needed for time-scheduling at the BS, such as how much data will be transmitted, the maximum possible data rate at which the mobile can work based on current mobile available power. The R-REQCH can be transmitted periodically or when there is new data arrival into the mobile's buffer. The BS uses the Forward Grant Channel, to inform the MS of scheduling grant information.

- **Handover**

The Handover or Handoff (HO) means the process that the existing connection in current cell is torn down and a new connection in the proper cell is established without losing the ongoing connection. HO is one of the essential means that guarantees user mobility in a mobile communication network. It aims to provide the service continuity to mobile users who are moving over cell boundaries. In UMTS systems, we have hard handover, soft handover, and softer handover (Harry & Toskala 2000). Hard handover means that the old connections are removed before the new links are established; soft handover occurs when the mobile is in the overlapping area of two adjacent cells; softer handover is a special case of soft handover that the soft handover occurs when the old link and the new one belong to the same base station.

- **Beamforming**

Beamforming, Adaptive antennas, or Smart antennas, is of importance to radio communications, which is a technique for spatial filtering of radio signals in antenna arrays. The main objective of beamforming is to adjust complex weights connected to every antenna branch to reshape the receiver antennas' radiation pattern to a certain shape which achieves the required objective, for instance, to maximize the received SINR. The performance enhancement of the beamforming can be achieved by spatial processing, which depends on the phase differences of received signals between the antenna components. And also it can be improved by exploiting the delay spread of the received multipath signals, by which one desired path signal is received and the others are ignored. The beamforming can be done in both receiving and transmitting arrays.

In this thesis, we mainly discuss the power control schemes. For the others, there are many excellent materials, such as (Elmusrati 2004), (Hasu 2007), (Jäntti 2001), (Tse & Viswanath 2005).

5. POWER CONTROL

The transmitter power control is an essential technique to balance the received signal strength and the interference power, which allows devices to setup and maintain wireless links with minimum power to meet the target signal-to-interference noise ratio (SINR). Power control has a number of benefits, for instance, mitigate the near-far problem, increase the capacity of the system through effective interference mitigation, prolong the battery life of the mobile terminal, improve the service quality, and others.

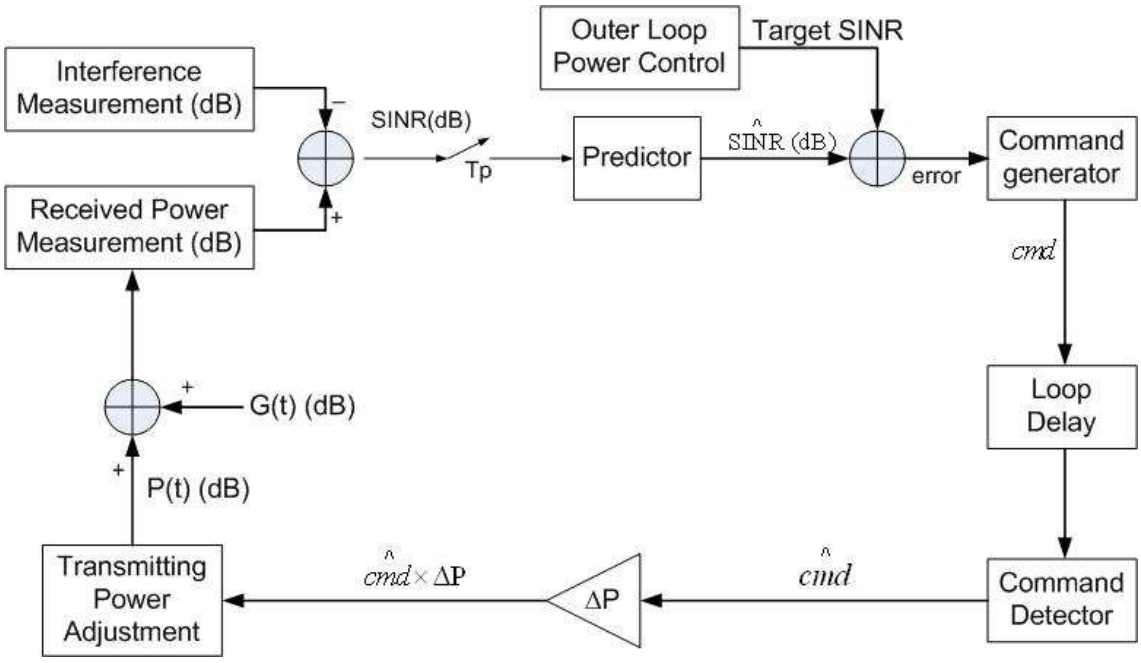

Figure 5.1: The Conventional Received SINR Prediction-based Power Control (Harry 2000).

There are three power control schemes, called open-loop power control, closed-loop power control and outer-loop power control. All three power control schemes are used in uplink while the later two are used in downlink. Open-loop power control is the

ability of user to set its initial transmission power. During user random access procedure, BS measures the SINR of the uplink signal. Then it will decide what transmission power the user should use to achieve the target SINR and then send an adjustment command to the user. According to the update command, the user will set its output power in the next uplink updating time slot. Closed-loop power control is the ability of user/BS to adjust its transmission power according to the Transmit Power Control (TPC) command received in downlink/uplink. According to what we introduced in wireless communication part of this these, because of the varying nature of wireless channel and user mobility, the received signal quality at base station (BS) will vary with time. In order to match the target SINR at the receiver, BS must periodically send TPC to the user and user adjusts its output power. Outer-loop power control is the ability of user/ BS to adjust the target SINR by calculating the received Frame Error Rate (FER). If the received FER is higher than a predetermined threshold a higher target SINR is increased. In this section we will introduce some basic power control schemes: why we should utilize power control schemes, what are the basic and important power control algorithms, and how to use power control in some very bad channel conditions, for instance, low correlated fading channel and uncorrelated fading channel.

5.1 An Introduction to Power Control

Transmission power control is a key technique for the resource allocation of wireless radio communication networks. As we know that a scarce radio spectrum imposes great limitations on the design of cellular radio systems. Consequently, in order to provide communication services with a high capacity and a good quality of service requires efficient methods for sharing the radio spectrum. In practice, all sharing methods introduce interference which is proportional to the transmitter powers. As we know that the Signal to Interference and Noise Ratio (SINR) at the receiver (here we do not consider the processing gain) is given by

$$\Gamma = \frac{G_{ii} P_{ii}}{\sum_{j \neq i}^{N} G_{ij} P_{ij} + N_i} \tag{5.1}$$

where G_{ij} is the channel gain and P_{ij} is the transmitted power from the transmitter *j* to receiver *i*, and N_i is the noise at receiver *i*. From this equation it is obviously how the interferences of different transmitters interact. Next we will illustrate how important the transmission power control is by using a simple example known as near-far problem.

5.1.1 Near-Far Problem

Let us consider the situation depicted in Fig. 5.2, which is a non-orthogonal system without power control scheme utilized. Mobile 1 and mobile 2 share the same frequency band and their signals are separable at the base station by their unique spreading codes. The signal of the terminal with highest link quality will overpower the others, which is known as near-far problem. Next we will show a simple example mathematically how the worse signals are overpowered.

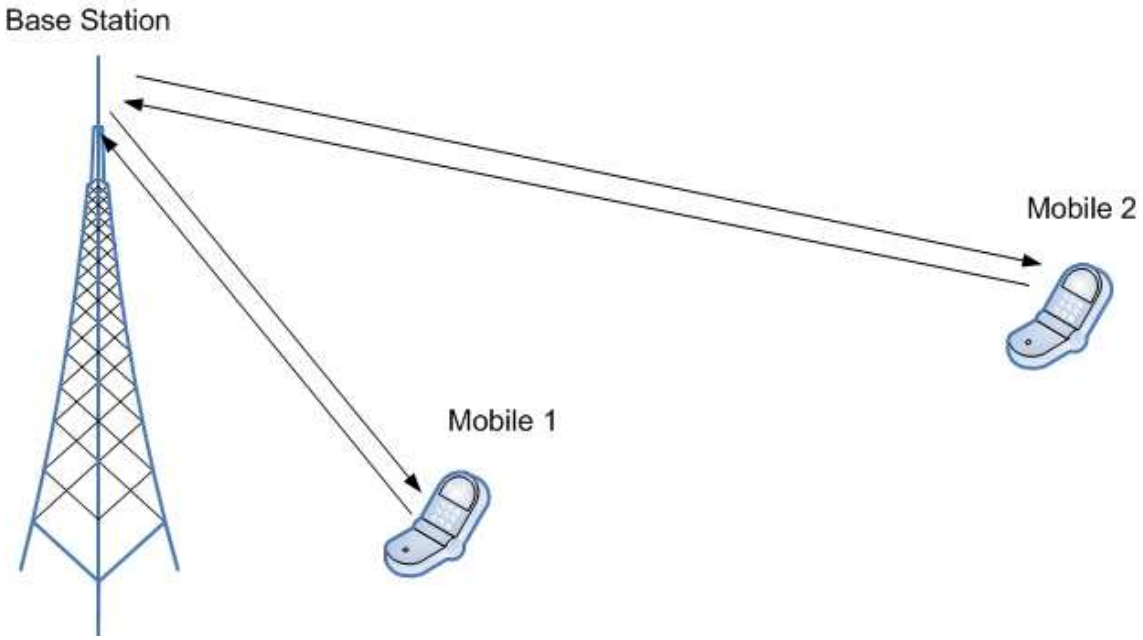

Figure 5.2: Near-far Problem.

Example: In figure 2.2, the channel gain follows $G_i = \frac{1}{d_i^4}$, where d_i is the distance between mobile i and the base station, d1 = 30m and d2 = 100m. The noise is $7\times10^{-14}w$, the transmit power of each mobile is 0.2w, and the minimum required SINR for each mobile is −7dB.

Solution: By using the given values in above description, first we calculate the channel gain for each link.

$$G_1 = \frac{1}{d_1^4} = \frac{1}{30^4} = 1.2346\times10^{-6}$$

$$G_2 = \frac{1}{d_2^4} = \frac{1}{100^4} = 10^{-8}$$

Then according to equation (5.1), we can compute the SINR at the receiver for each mobile.

$$\begin{aligned}\Gamma_1 &= \frac{G_1 P_1}{G_2 P_2 + N} \\ &= \frac{1.2346\times10^{-6}\times0.2}{10^{-8}\times0.2+7\times10^{-14}} \\ &= 123.4557\end{aligned}$$

In *dB* scale, $\Gamma_1 = 48.1588\ dB$. And,

$$\begin{aligned}\Gamma_2 &= \frac{G_2 P_2}{G_1 P_1 + N} \\ &= \frac{10^{-8}\times0.2}{1.2346\times10^{-6}\times0.2+7\times10^{-14}} \\ &= 0.0081\end{aligned}$$

In *dB* scale, $\Gamma_2 = -48.1592\ dB$.

From this simple example, even though the two mobiles transmit using the maximum values of transmission power, the second signal is overpowered by the first one, and only the first one can achieve the minimum required SINR to be able to access the network.

5.1.2 Open Loop Power Control

Open loop power control is the ability of the user equipment (UE) transmitter to set its initial transmission power to a specific value, for at this time the two-way communication link has not been established and also the closed loop is not available. The initial level of the transmission power is based on estimating the pilot signal and does not require any feedback measurement on the transmitter signal quality at the receiver. However, due to the frequency separation, the uplink and downlink channels have different channel conditions, which mean that the correlation between up- and downlink attenuations is generally weak. In addition, the rapid variations of the wireless channels cause the received signal to change fast constructively and destructively. In

this case the open loop power control just makes things worse. Therefore, the transmission power update of a mobile must be based on feedback information of the received SINR at the base station, which is the function of a closed loop power control between them and the open loop power control is not used once the closed loop power control is running (Harry & Antti 2000). The Fig. 5.3 illustrates different types of the power control mechanisms in WCDMA systems.

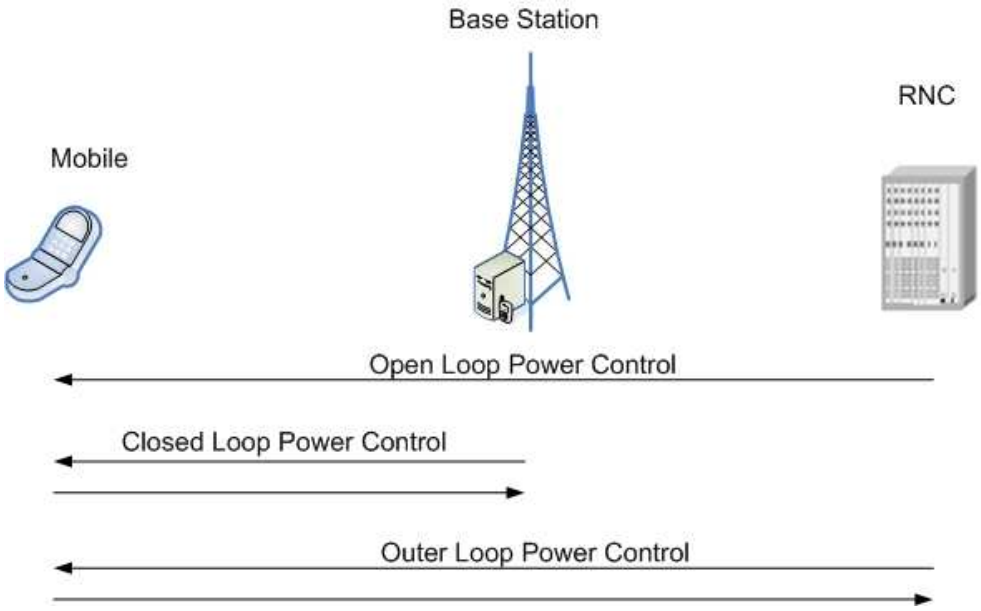

Figure 5.3: WCDMA Power Control Schemes (Harry & Antti 2000; Pristinsky 2002).

5.1.3 Closed Loop Power Control

When the radio connection is established the power control method is changed. During the connection the Closed Loop Power Control method is used while the open loop power control is only used when the mobile is inactive and tries to get a connection. Within this method the base station (BS) commands the mobile either increase or decrease its transmission power with the pace of 1.5 kHz in WCDMA systems (Harry & Antti 2000). The decision whether to increase or decrease the power is based on the received SIR estimated by the BS. A closed-loop power control normally can be divided

into two types, fixed-step and adaptive-step. In a fixed-step size closed-loop power control system, the base station measures the received signal power which is the power of the combination of the multipath signals, and then compares it with a target power provided by the outer loop power control system. After the comparison, a command bit is generated which is logical ’1’ if the received power is less than the target value or ’0’ for others. The transmitter adjusts its transmission power value according to the command bit with a fixed step value. In an adaptive-step size closed-loop power control system, the mobile adjusts its power update step size automatically according to the pattern of its received power control bits. For instance, a new adaptive power control, Mobility Based Adaptive Closed-loop Power Control (M-ACLPC) Scheme, was proposed in (Lee & Cho 2003), where the scheme selects the power control step size by considering the speed of the mobile station and a variable step size by using instantaneous companding logic based on power control command bit patterns. The block diagram of M-ACLPC algorithm is illustrated in Fig. 5.4, the multiplication factor for determining the adaptive step-size is showed in Tab. 5.1.

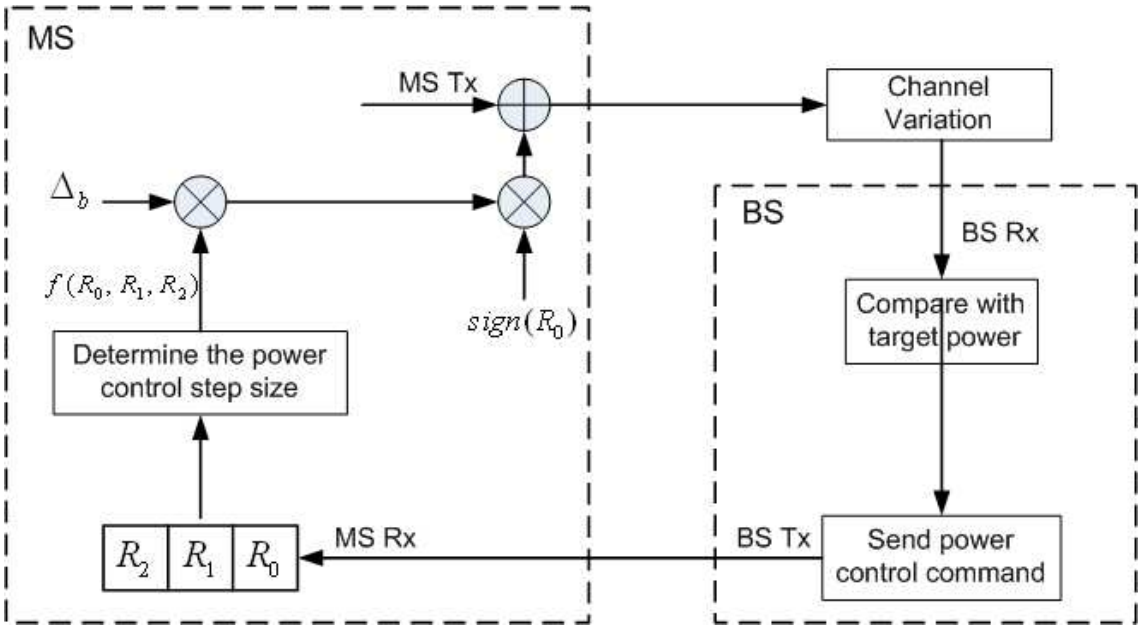

Figure 5.4: Block Diagram of M-ACLPC with Adaptive Step Size (Lee & Cho 2003).

Table 5.1: Multiplication Factor used for Determining Adaptive Step Size

R2	R1	R0	f(R0,R1,R2)
0	0	0	1.5
1	0	0	1
1	1	0	0.66
0	1	0	0.66
1	1	1	1.5
0	1	1	1
1	0	1	0.66
0	0	1	0.66

The algorithm is given as

$$P(t) = P(t - T_p) + sign(R_0)\left[\Delta_b \times f(R_0, R_1, R_2)\right] \tag{5.2}$$

where R_0 is the current power control command bit, and R_1 and R_2 are the previous power control command bits which are stored at the shift register of the mobile station and are used to decide the power control step size; Δ_b is the basic step size relative to the mobile speed, and $f(R_0, R_1, R_2)$ is a multiplication factor determined by the logic rule given by Tab. 5.1 ; T_p is the power control period and $sign(\cdot)$ is the sign function.

5.1.4 Outer Loop Power Control

The outer loop power control is needed to keep the quality of communication at the required level by setting the target for the fast power control (Harry & Antti 2000: 140). The outer loop aims at providing the required quality: no worse, no better. Too high quality would waste capacity. The outer loop is needed in both uplink and downlink because there is fast power control in both uplink and downlink. In UMTS systems, the

uplink outer loop is located in RNC and the downlink outer loop in the user equipment (UE). The target SINR is updated for each UE according to the estimated uplink quality (Frame Error Ration, Bit Error Ratio) for each Radio Resource Control connection. The downlink outer loop power control is the ability of the UE receiver to converge to the required link quality (BLER) set by the network (RNC) in downlink. The Fig. 5.5 gives a general outer loop power control algorithm (Harry & Antti 2000: 150).

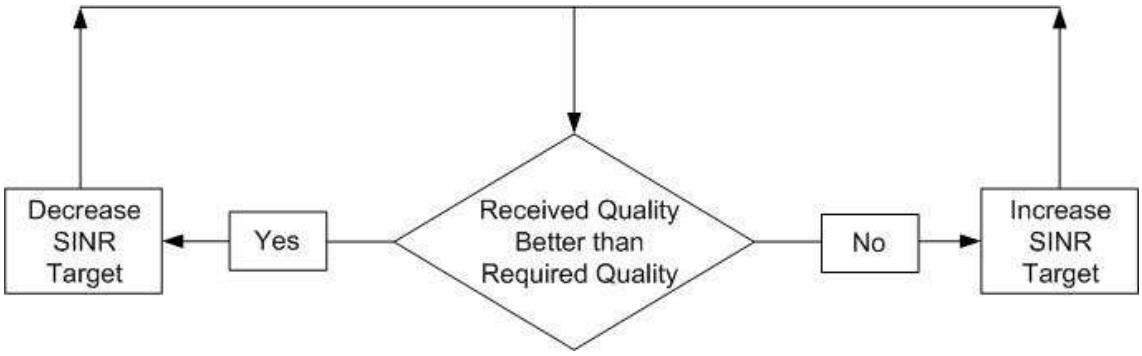

Figure 5.5: General outer loop power control algorithm.

5.2 Power Control Algorithms

5.2.1 Centralized Power Control

In this section, the centralized power control scheme is presented in order to further study the other power control algorithms, even though the centralized power control has some limitations and is not suitable to practical uses. For this scheme, all the information of all channel gains and transmission powers should be known.

For the sake of simplicity, we can assume the worst case that the orthogonal factor θ_{ij} between the signals is 1.

$$\Gamma_i = \frac{P_i G_i}{\sum_{\substack{j=1 \\ j \neq i}}^{M} P_{ij} G_{ij} + N_i} \geq \Gamma_i^T \tag{5.3}$$

Then the transmit power of terminal i is as following

$$P_i \geq \Gamma_i^T \left[\sum_{\substack{j=1 \\ j \neq i}}^{M} P_j \frac{G_{ij}}{G_i} + \frac{N_i}{G_i} \right] \tag{5.4}$$

In order to obtain the matrix form and the transmit power be minimum value, expression (7.2) can be rewritten to

$$P_i - \Gamma_i^T \sum_{\substack{j=1 \\ j \neq i}}^{M} P_j \frac{G_{ij}}{G_i} = \Gamma_i^T \frac{N_i}{G_i} \tag{5.5}$$

Then the matrix form comes to

$$\left[\mathbf{I} - \Gamma^T \mathbf{H} \right] \mathbf{P} = \mathbf{u}, \tag{5.6}$$

where **I** is the identity matrix, Γ^T is the target signal-to-noise ratio, **P** is the transmit power matrix, **u** is a vector with positive elements u_i given by

$$u_i = \frac{\Gamma_i^T N_i}{G_i}, \qquad i = 1, 2, ..., M \ , \tag{5.7}$$

and **H** is a nonnegative matrix with the elements as following

$$H_{ij} = \begin{cases} 0, & i = j \\ \dfrac{G_{ij}}{G_i}, & i \neq j \end{cases} \tag{5.8}$$

Next let $\rho(\mathbf{H})$ be the spectral radius of matrix **H**, which is the maximum eigenvalue of **H**. Then according to (Gantmacher 1964; Grandhi et al. 1993), when

$$\Gamma_T < \frac{1}{\rho(\mathbf{H})} \quad , \tag{5.9}$$

the linear system of equations given by (5.6) has a unique positive power vector solution, also the optimal power solution

$$\mathbf{P}^* = \left[\mathbf{I} - \Gamma^T \mathbf{H}\right]^{-1} \mathbf{u} \tag{5.10}$$

Example: In this example, we solve the near-far problem presented in the previous subsection, and all the parameters are same.

Solution:

First, formulate the **H** matrix:

$$\mathbf{H} = \begin{bmatrix} 0 & \frac{G_2}{G_1} \\ \frac{G_1}{G_2} & 0 \end{bmatrix} = \begin{bmatrix} 0 & \frac{30^4}{100^4} \\ \frac{100^4}{30^4} & 0 \end{bmatrix} = \begin{bmatrix} 0 & 0.0081 \\ 123.4568 & 0 \end{bmatrix}$$

Second, formulate the **u** matrix:

$$\mathbf{u} = \begin{bmatrix} \frac{\Gamma^T N}{G_1} \\ \frac{\Gamma^T N}{G_2} \end{bmatrix} = \begin{bmatrix} \frac{10^{-0.7} \times 7 \times 10^{-14}}{1/30^4} \\ \frac{10^{-0.7} \times 7 \times 10^{-14}}{1/100^4} \end{bmatrix} = \begin{bmatrix} 1.1313 \times 10^{-8} \\ 1.3967 \times 10^{-6} \end{bmatrix}$$

Then we can calculate the optimal transmit power for each mobile to achieve the required SINR by using the equation (5.10)

$$\mathbf{P}^{*} = \left[\mathbf{I} - \Gamma^{T}\mathbf{H}\right]^{-1}\mathbf{u}$$

$$= \left(\begin{bmatrix} 1 & 0 \\ 0 & 1 \end{bmatrix} - 10^{-0.7}\begin{bmatrix} 0 & 0.0081 \\ 123.4568 & 0 \end{bmatrix}\right)^{-1}\begin{bmatrix} 1.1313\times10^{-8} \\ 1.3967\times10^{-6} \end{bmatrix}$$

$$= \begin{bmatrix} 0.0118\times10^{-6} \\ 1.3967\times10^{-6} \end{bmatrix}$$

In consequence, from this quite simple example we can find that the values of optimal transmit power are extremely low, but the two terminals can achieve the required SINR. Also it indicates that the power control scheme is of importance to optimize our systems.

5.2.2 Two-User power control

In this subsection, we will use a graphical way to illustrate the power control problem. Let assume that g_i, i = 1, 2, is the channel gain for user i, p_i is the transmission power value of user i, Γ^T is the target SINR, and $p_{\max}$ is the maximum transmit power of two users. According to the centralized power control algorithm presented previously, we obtain

$$\frac{p_1(t)g_1(t)}{p_2(t)g_2(t)+N} \geq \Gamma^{T} \tag{5.11}$$

$$\frac{p_2(t)g_2(t)}{p_1(t)g_1(t)+N} \geq \Gamma^{T} \tag{5.12}$$

Then we can achieve

$$p_1(t) \geq \Gamma^T \frac{g_2(t)}{g_1(t)} p_2(t) + \frac{N\Gamma^T}{g_1(t)} \tag{5.13}$$

$$p_2(t) \geq \Gamma^T \frac{g_1(t)}{g_2(t)} p_1(t) + \frac{N\Gamma^T}{g_2(t)} \tag{5.14}$$

According to equations (5.13, 5.14), we can draw the Fig. 5.6. In the shadowed area, the SINR two users obtained can be larger than target SINR, and the intersection point is the optimal power. We also can draw another conclusion that if the user 1 want to increase its SINR in order to achieve higher data rate, the slop of line 1 will increase, while if user 2 want to increase its SINR in order to achieve higher data rate, the slope of line 2 will decrease. However, the intersection of two lines can not be out of the area $p_{\max} \times p_{\max}$. Otherwise, one user will be out of service.

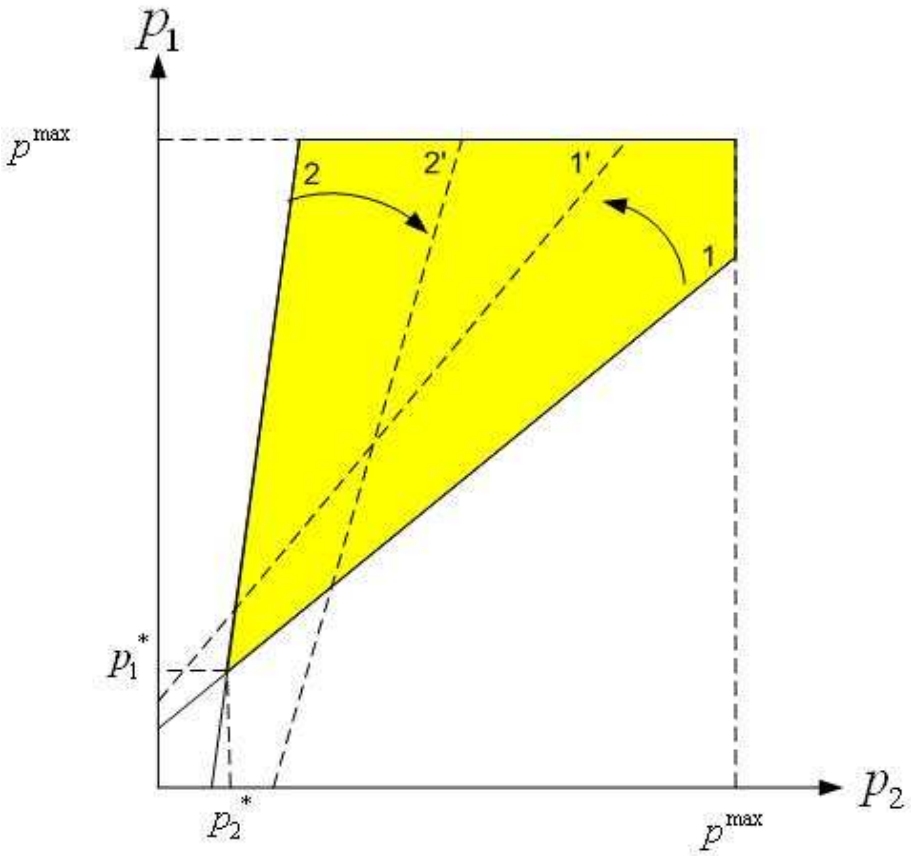

Figure 5.6: Two-User Power Control.

5.2.3 Distributed Power Control

The distributed power control scheme only needs the local information for a transmitter using a optimal value of power to transmit, therefore it can overcome the limitations/difficulties encountered in centralized power control. In consequence, distributed power control plays a key role in current wireless communication systems, for instance CDMA, wireless Ad Hoc networks, and others. Up to now, many experts have contributed a number of distributed power control algorithms which are theme-varying based on setting the new power level according to the experienced/measured SINR between the transmitter and receiver. These algorithms include distributed balancing algorithm (DBA) (Zander 1992), distributed power control (DPC) (Grandhi et al. 1994), Foschini and Miljanic algorithm (FMA) (Foschini & Miljanic 1993), second order power control (SOPC) (Jäntti & Kim 2000), and PI power control (PIPC) (Uykan et al. 2000), multi-objective distributed power control (Elmusrati & Koivo 2002), and others. However, in this section only some classic/general algorithms are introduced.

A. Iterative Methods

As the power control problem can be modeled as a linear system, the distributed power control algorithms can be obtained by using iterative methods to solve a linear system mathematically. Thus we show some iterative methods in order to familiar how to derive the classic distributed power control algorithm using the iterative ways.

Jacobi Method: The Jacobi method is a method of solving a matrix equation on a matrix that has no zeros along its main diagonal. Each diagonal element is solved for, and an approximate value plugged in. The process is then iterated until it converges. The Jacobi method is easily derived by examining each of the n equations in the linear system of equations **AX=b**. Let the ith equation be

$$\sum_{j=1}^{n} a_{ij} x_j = b_i . \tag{5.15}$$

Then the Jacobi Method comes to

$$x_i^{(k)} = \frac{b_i - \sum_{j \neq i} x^{(k-1)}_j}{a_{ii}}, \tag{5.16}$$

where the other entries of x are assumed to remain fixed. (Mathworld 2008).

Gauss-Seidel Method: The Gauss-Seidel method is another technique for solving the linear system of equations AX=b. Gauss-Seidel Method is given by

$$x_i^{(k)} = \frac{b_i - \sum_{j<i} a_{ij} x_j^{(k-1)}}{a_{ii}} \tag{5.17}$$

Gauss-Seidel method has two essential characteristics. First, the computations appear to be serial, that is the updates cannot be done simultaneously as in the Jacobi method or each component of the new iterate depends upon all previously computed components. Second, the new iterate depends on the order in which the equations are examined. If this ordering is changed, the component of the new iterates will also be changed. (Mathworld 2008).

Successive Overrelaxation Method: The successive overrelaxation method (SOR) is an additional method used to solve a linear system of equations **AX=b** derived by extrapolating the Gauss-Seidel method. This extrapolation takes the form of a weighted average between the previous iterate and the computed Gauss-Seidel iterate successively for each component, which is given by

$$x_i^{(k)} = \omega \bar{x}_i^{(k)} + (1-\omega) x_i^{(k-1)} \tag{5.18}$$

where $\bar{x}$ denotes a Gauss-Seidel iterate and ω is the weighted factor. The idea is to choose a value for ω to accelerate the convergence rate of the iterative processes. (Mathworld 2008).

B. Get the Classic DPC Algorithm

From expression (5.3), it is easy by equalizing it to get the following equation

$$P_i = \frac{\Gamma_i^T \left(\sum_{j \neq i} P_j G_{ij} + N_i \right)}{G_i} \tag{5.19}$$

By utilizing the Jacobi method, P_i can be updated iteratively at iteration k as

$$P_i(k+1) = \frac{\Gamma_i^T \left(\sum_{j \neq i} P_j(k) G_{ij} + N_i \right)}{G_i} \tag{5.20}$$

Then we can gain the following equation by multiply $P_i(k)$ to the numerator and the denominator of equation (5.20),

$$P_i(k+1) = \frac{\Gamma_i^T \left(\sum_{j \neq i} P_j(k) G_{ij} + N_i \right) P_i(k)}{G_i P_i(k)} \tag{5.21}$$

From equation (5.3) we know that the SINR at iteration k is given by

$$\Gamma_i(k) = \frac{G_i P_i(k)}{\sum_{j \neq i} G_{ij} P_{ij}(k) + N_i} \tag{5.22}$$

In consequence, the equation (5.21) can be rewritten as

$$P_i(k+1) = \frac{\Gamma_i^T}{\Gamma_i(k)} P_i(k), \tag{5.22}$$

which is the classic distributed power control algorithm. From it we can find that the current and the target SINRs are the only parameters needed to know in order to update the transmit power in next iteration.

C. How does the Classic DPC Algorithm work

1. The transmitter utilizes a initial transmit power, $P_i(0) \geq 0$, which is should be high enough in order to the receiver can recognize it.

2. The receiver estimates the received SINR, and also compares it to the target SINR, then informs the transmitter through a feedback channel.

3. The transmitter update it's transmit power according to equation (5.22).

4. Go to step 2.

5.2.4 Distributed Constrained Power Control

The DPC algorithm introduced in previous subsection does not consider the upper-bound of the maximum output of a transmitter. However, in practice the maximum output power is constrained in order to prolong the battery life as well as reduce the interference to other devices. Grandhi et al. (1995) showed that the constraints do not induce any stability problems. Let the constraint of the transmit power be

$$0 \leq P \leq P_{max} \tag{5.23}$$

Then the DPC algorithm (5.22) can be represented as following

$$P_i(k+1) = min\left(P_{max}, \quad \frac{\Gamma_i^T}{\Gamma_i(k)} P_i(k) \right) \tag{5.24}$$

This algorithm is called Distributed Constrained Power Control (DCPC) (Grandhi et al. 1995), which the transmitter updates its power according to DPC algorithm, but when the required power from DPC power is greater then the maximum power $P_{\max}$, the transmitter uses $P_{\max}$ to transmit.

5.3 Dynamical Effects of Time Delays to Power Control

Gunnarsson et al. (2001) presented the dynamical effects of time delays to implementing transmission power control in DS-CDMA systems. This kind of effect also exists in other wireless communication systems, for instance, wireless ad hoc networks. We know that for all the three types of power control, the system needs to measure the received the SINR, and also sending the updating commands takes time. All these result in power control delays. Consequently, the accuracy of power control scheme used to negotiate/mitigate the effects due to channel variation will decrease. In addition, Sim et al. (1998) showed that power control is more sensitive to the delay than to the SINR estimator performance. Thus it is importance of analyzing the dynamical effects of time delays. In next example, we show the effects of power control delay in a time-varying wireless channel.

Example: Assume that the transmission time interval (TTI) is 2ms and the channel quality indicator feedback delay is 4ms. Also the mobile speed is at 120km/h, and the carrier frequency is 1.8GHz.

Answer: According to the previous sections, the Doppler spread can be obtained approximately

$$D_s = \frac{vf_c}{c} = \frac{\frac{120\times10^3}{3600}\times1.8\times10^9}{3\times10^8} = 200Hz\,.$$

Then the relative coherence time of the channel is

$$T_c \approx \frac{1}{D_s} = \frac{1}{200} = 5ms\,.$$

We can find that the summation of feedback delay and the TTI approximate the channel coherence time. Therefore, in this case the power control commands will become outdated or can not track the fast fading any more. In order to track the fast fading, many authors have contributed numerous approaches for predicting and compensation the time delay in power control scheme.

5.4 Lee's DPC in Fading Channels

In this section we will introduce three distributed power control schemes in fading channels done by Lee and Park (2002). The authors proposed a general DPC algorithm which is conformed to trace the target SINR efficiently in fading channel conditions. The SINR is presented just like we show previously as

$$\gamma_i(t) = \frac{g_i(t)\,p_i(t)}{I_i(t)} \tag{5.26}$$

where i(t) is the SINR value of the ith mobile, $g_i(t)$ is the channel loss link i between the transmitter i and receiver i, p_i is the transmit power of mobile i, and $I_i(t)$ is the total interference at receiver i which includes inter-cell, cross-cell interference, and

noise. Then the SINR variation is obtained by differentiating equation (5.22), where the transmit power $p_i(t)$ and the channel gain $g_i(t)$ are considered to be time varying, but the total interference is considered to be a constant. So the SINR variation comes to

$$\gamma_{i'}(t) = \frac{1}{I}\left[g_{i'}(t)\,p_i(t) + g_i(t)\,p_{i'}(t)\right] \tag{5.27}$$

where $\gamma_{i'}(t) = -\beta\left[\gamma_i(t) - \gamma^T\right]$ is the difference value of current SINR and target SINR. Then we can obtain the following equation

$$g_{i'}(t)\,p_i(t) + g_i(t)\,p_{i'}(t) = -\beta g_i(t)\,p_i(t) + \beta I\gamma^T \tag{5.28}$$

where β is a constant between 0 and 1 which controls the convergence rate of algorithm (Foschini & Miljanic 1993). By some simple linear function processing to equation (5.28) we can conclude

$$p_i'(t) = -\left[\beta + \frac{g_i'(t)}{g_i(t)}\right]p_i(t) + \frac{\beta\gamma^T I}{g_i(t)} \tag{5.29}$$

Now using the transformation from differential equation to discrete time domain, that is we have: $p_i'(t)$ is replaced by $p_i(k+1) - p_i(k)$, and $g_i'(t)$ is replaced by $g_i(k) - g_i(k-1)$. Therefore the equation (5.29) is transformed to

$$p_i(k+1) - p_i(k) = -\left[\beta + \frac{g_i(k) - g_i(k-1)}{g_i(k)}\right]p_i(k) + \frac{\beta\gamma^T I}{g_i(k)} \tag{5.30}$$

Then we can achieve the Lee's distributed power control algorithm as

$$p_i(k+1) = \left[-\beta + \frac{g_i(k-1)}{g_i(k)} + \beta\frac{\gamma^T}{\gamma(k)}\right]p_i(k) \tag{5.31}$$

From above algorithm, we can find that if the convergence coefficient $\beta = 1$, and the channel gain *g(t)* is a constant, Lee's algorithm becomes to the classical DPC algorithm

$$p(k+1) = \frac{\gamma^T}{\gamma(k)} p(k). \tag{5.32}$$

5.5 Power Control for Low Correlated Fading Channels

From previous analysis, we have achieved that the most important characteristics of wireless or radio channels are time delay and time varying. We also have studied the effects caused by them through proposing some simple examples, which conclude that kinds of effects will result in numerous disadvantages. For instance, the increase of interference, difficulties of tracking the channel variations in order to transmit with optimal power value, QoS (Quality of Service) decreasing, shorten lifetime of battery especially for mobile users, and so forth. In addition, we also introduced some power control schemes for optimizing transmission power. For classical Distributed Power Control Algorithm (DPC), it assumes that the radio channel is highly correlated, which means the channel gain approximately keeps constant in adjacent power update intervals. Under this condition, DPC runs very nice. In this section we will discuss the worse case which affects the transmission control schemes.

In this part, low correlated radio channels are considered. Under this assumption, the current channel information will not be predicted accurately. The channel information is not so helpful to the next power control interval. Consequently, the received signal-to-noise ratio (SINR) for users will also vary unpredictably. SINR is the essential parameter for receivers to recover the transmitted signals. Thus we have to modify the classical DPC scheme in order to track, to some degree, the channel variations.

5.5.1 Correlated Channel Model Based on Channel Correlation

As what we discussed in previous sections, correlation is a matching process. Autocorrelation refers to the matching of a signal with a delayed version of itself. In another word, $R_x(\tau)$ is not a function of time, but only a function of the time difference τ between the waveform and its shifted copy. $R_x(\tau)$ provides a measure of how closely the signal matched a shifted τ-unit copy in time. Therefore, we can say if the shifted copy only matches a little, then it is low correlated. This results in only a little old information is carried by the shifted copy. From the power control's point of view, only small partial information of the time-varying channel can be used to power control algorithms for next update step.

We have showed in previous chapter,

$$g_i(t) = L_i(t) \cdot S_i(t) \cdot FF_i(t) \tag{5.33}$$

where $g_{ij}(t)$ is the time-varying channel gain, $L_i(t)$ is path loss, $S_i(t)$ means shadow fading following log-normal distribution, and $FF_i(t)$ is the power attenuation caused by fast multipath fading. In (5.32), items are obtained by

$$L_i(t) = \frac{1}{d^4} \tag{5.34}$$

$$S_i(t) = 10^{(N \cdot \sigma_s / 10)} \tag{5.35}$$

where d is the path distance between transmitter and receiver, N is a standard normal distributed variable, and σ_s^2 is the log variance of variable $S_i(t)$. And for $FF_i(t)$ is the power attenuation, $\sqrt{FF_i(t)}$ is the envelope of received signal.

To model the time-variant link gains, we use the following model,

$$\hat{g}_i(t+1) = R^2 g_i(t) + (1-R^2)\cdot\chi \tag{5.36}$$

where R is the correlation coefficient, and χ is a random variable with the same distribution as $g_i(t)$.

In the following analysis, we assume that our system encounters Rayleigh-distributed fast fading. Therefore, the received signal envelope is Rayleigh distributed, and channel gain, of course, follows Exponential distribution. Let the Exponential distribution parameter is λ. Thus the mean value in time slot *t* of channel gain is

$$\overline{g(t)} = \frac{1}{\lambda}. \tag{5.37}$$

Please notice that here we use $\overline{g(t)}$ as the mean value in time slot *t.* However, at another time slot, we have different value. In addition, this expected channel gain depends on the distance-based path loss and shadow fading. That is

$$\overline{g(t)} = \frac{S}{d^4} \tag{5.38}$$

where S is the shadow fading, and d is the distance between the transmitter and the receiver. Here, we use the common value, 4, for the distance exponential factor. Moreover, this mean value is used for generating the exponential distributed fast fading.

The received signal to noise ratio at the receiver follows

$$\hat{\Gamma}_i(t+1) = R^2\Gamma_i(t) + (1-R^2)\cdot\chi_\Gamma \tag{5.39}$$

where $\hat{\Gamma}_i(t+1)$ is the predicted received SINR in time slot $(t+1)$, $\Gamma_i(t)$ is the measured SINR at time slot t, R is the correlation coefficient, and the χ_Γ is a random variable

with the same distribution with $\Gamma_i(t)$. From Ahmed & Elsayes (2002), we know that the Lognormal distribution can be utilized to model the received SINR' distribution.

5.5.2 Power Control Model Based on Channel Correlation

As we have studied previously, the classical distributed power control (DPC) is given

$$p_i(t+1) = \frac{\Gamma^T}{\Gamma_i(t)} p_i(t) . \tag{5.40}$$

From previous analysis in this chapter, we know that the current measured $\Gamma_i(t)$ can not well be used to compute the predicted transmit power for next updating. Here, we will use the proposed model (5.39) to predict the SINR in next time slot. Therefore the equation (5.40) becomes

$$\hat{p}_i(t+1) = \frac{\Gamma^T}{\hat{\Gamma}_i(t+1)} p_i(t) \ , \quad \text{and} \quad \hat{\Gamma}_i(t+1) = R^2\Gamma_i(t) + (1-R^2)\cdot\chi_\Gamma \tag{5.41}$$

This algorithm works as following (only theoretically):

- The current received SINR is measured at the receiver.
- The predicted transmission power for next time slot is computed by $\hat{\Gamma}_i(t+1) = R^2\Gamma_i(t) + (1-R^2)\cdot\chi_\Gamma$, χ_Γ is the generated random number following lognormal distribution.
- Compare the predicted SINR with the target SINR, if $\hat{\Gamma}_i(t+1) > \Gamma^T$, the transmission power will be increased in next time slot. Otherwise, it is decreased.

Next we analyze the power update according to channel correlation from another aspect. Following the subsection (5.5.1), we can calculate the predicted SINR as following.

We know that

$$\Gamma_i(t) = \frac{g_i(t)\,p_i(t)}{I_i(t)} \tag{5.42}$$

and

$$\begin{aligned} I_i(t) &= \sum_{j \neq i} g_j(t)\,p_j(t) + N_i \\ &= I_{total}(t) - g_i(t)\,p_i(t) \\ &= \sum_k g_k(t)\,p_k(t) + N_i - g_i(t)\,p_i(t) \end{aligned} \tag{5.43}$$

Because the interference is also time-varying, we can rewrite the interference $I_i(t)$ to predicted interference $\hat{I}_i(t+1)$ as

$$\hat{I}_i(t+1) = R^2 I_i(t) + (1-R^2)\chi_I \tag{5.44}$$

where $\chi_I = \sum_k \hat{g}_k(t+1)\,p_k(t) + N_i - \hat{g}_i(t+1)\,p_i(t)$. Then equation (5.40) becomes to

$$\begin{aligned} \hat{p}_i(t+1) &= \frac{\Gamma^T}{\hat{g}_i(t+1)}\hat{I}(t+1) \\ &= \frac{\Gamma^T}{\hat{g}_i(t+1)}\left(R^2 I_i(t) + (1-R^2)\chi_I\right) \end{aligned} \tag{5.44}$$

5.5.3 Numerical Results and Conclusion

In this simulation, we assume that there are 10 mobiles randomly distributed around one base station with a distance from 20 to 200 meters. The distance exponent factor is 4, and the noise power is set to −110dBm. The target received SINR is -12dB. The log-normal shadow fading has a 0dB mean and 6dB variance. The received signal envelope is following Rayleigh distribution. In this case, we do not consider the processing gain. Also assume that the distances between the mobile and the base station are fixed. Therefore, the channel gains for different links are exponentially distributed with mean values $\overline{g_i(t)} = \frac{S_i(t)}{d_i^4}$. This values are used to generate the channel gains in each time slot for link *i*.

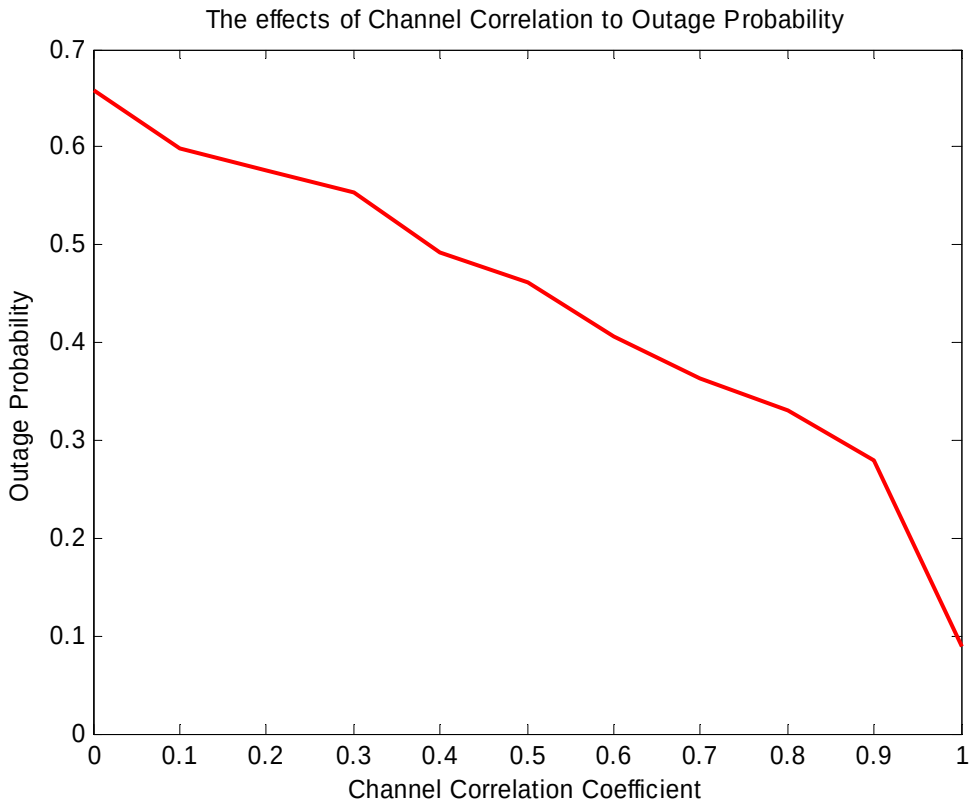

Figure 5.7: The effects of Channel Correlation to Outage Probability.

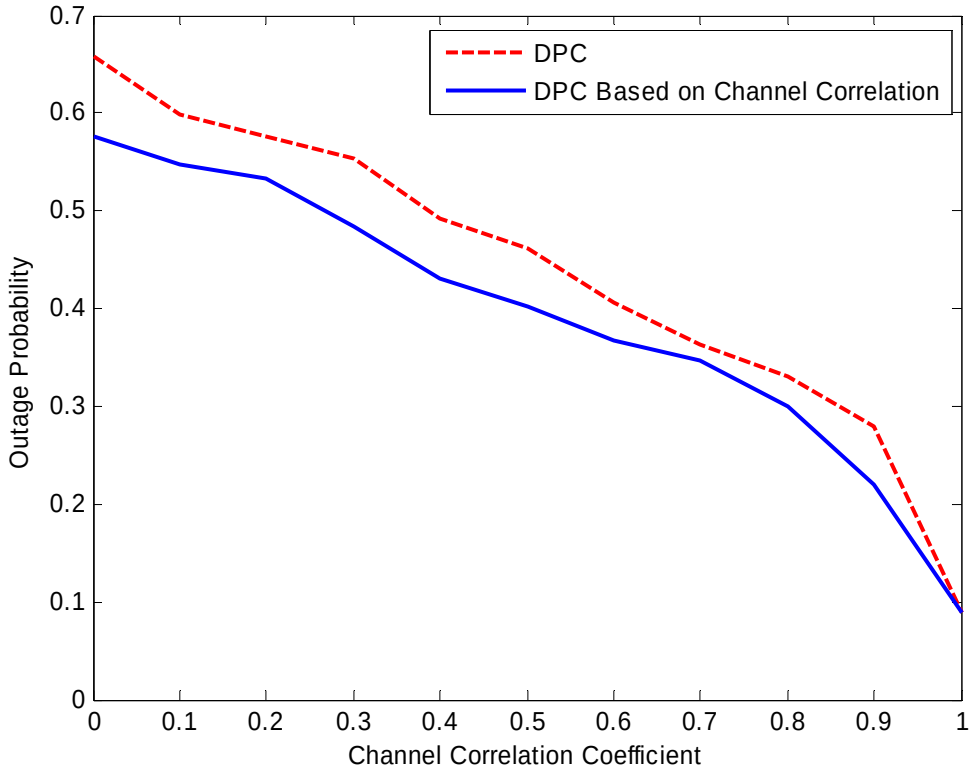

Figure 5.8: The comparison of Outage Probability Between DPC and DPC Based on Channel Correlation.

From above figures, we can notice that when the channel correlation coefficient decreases, the user average outage probability will increase. Because, the channel correlation decides how close the signal and its copy between the adjacent time slots are. In addition, from Fig. 5.8, we know that the DPC Based on Channel Correlation scheme has a little bit better outage probability. And also, with the decreasing of channel correlation, the benefit of DPC scheme based on channel correlation in time also has been increased.

5.6 Random Power Allocation for Uncorrelated Rician Fading Channels

In Previous section we consider the channel is low correlated, and present some analysis on that case. Now, the uncorrelated Rician fading channel is considered where the current channel measurement information is useless for power control updating. We utilize and analyze the random power allocation at the terminal where the transmit power is generated for each time slot following the proposed probability density function. Also the truncated inverted non-central chi-square distribution is used for generating random power. However, because the channel gains and transmitted power are random, the received power and the interference at the receiver are of course random. Next we discuss the random power allocation for uncorrelated Rician fading channels from several aspects: power allocation system model, mathematic analysis, and simulation.

5.6.1 Power Allocation Model for Uncorrelated Channels

As we showed previously, the probability density function (PDF) of the received signal envelope is of importance to analyze of fading channel models, which is required to calculate the probability of outage, the fade duration, level crossing rates, and others (Stüber 2002: 50). Here we assume a multiuser and highly dynamic environment where the channel gain G_{ij} is an uncorrelated random process. The transmitted signals arrive at the receiver via multipath environments with a specular or LoS component. This is a Rician fading environment where the envelope of the superposition of the received signals follows Rician distribution and the received power follows non-central chi-square distribution. And also a slotted system is considered, that is, mobile terminal uses different power value in each time slot. Then we assume that the time slot will approximately be the channel coherent time, which means that the length of a time slot is short enough, such that we can ignore the effects of the variations of the shadowing fading and distance-based attenuation. However, the channel characteristics are uncorrelated. This scheme follows the idea proposed in (Elmusrati et al. 2007) to analyze the power control allocation for uncorrelated Rician fading channels.

Let I_i and N_i be the received interference and noise power respectively, and γ be the minimum required signal to interference noise ratio (SINR) at the receiver, which means that when the received SINR is less than γ, the received signal can not be decoded properly (here without loosing generality we ignore the processing gain and SINR margin). Therefore the outage probability can be

$$P_{out} = P_r \left\{ \frac{G_i P_i}{I_i + N_i} \le \gamma \right\} \tag{5.45}$$

where G_i is the channel gain between the transmitter i and the receiver i, P_i is the transmitted power by transmitter i, and the I_i is given by

$$I_i = \sum_{j \neq i}^{k} G_j P_j \tag{5.46}$$

where k is the number of the transmitters, and assume the worst case that the orthogonal factor θ_{ij} between the signals is 1.

5.6.2 Random Power Allocation for Uncorrelated Channels

Let the complex envelope of the received composition be $r(t) = r_I(t) + jr_Q(t)$. $r_I(t)$ and $r_Q(t)$ are independent identically distributed Gaussian random process with non-zero means m_I and m_Q respectively. Also assume that $r_I(t)$ and $r_Q(t)$ have the same variance σ^2. In this case, the instantaneous envelope of the superposition of the received multipath signals has a Rician distribution.

The link gain, defined as the fraction between the received power and the transmitted power, has a non-central chi-square distribution with two degree of freedom as following. The characteristic function of the link gain is given by

$$\Psi_G(s) = \frac{1}{1-2s\sigma^2}\exp(\frac{m^2 s}{1-2s\sigma^2}) \tag{5.47}$$

where $m^2 = m_I^2 + m_Q^2$ is the non-centrality parameter. Then the probability density function of G can be received by using inverse-Fourier transform to the characteristic function,

$$p_{G_{ij}}(g) = \frac{1}{2\sigma^2}\exp(-\frac{m^2+g}{2\sigma^2})I_0(\sqrt{g}\,\frac{m}{\sigma^2}), \qquad g \geq 0 \tag{5.48}$$

The cumulative distribution function (CDF) for the link gain, non-central chi-square with 2 digrees of freedom, is

$$F_{G_i j}(g) = 1 - Q_1(\frac{m}{\sigma}, \frac{\sqrt{g}}{\sigma}), \tag{5.49}$$

where $Q_m(\cdot)$ is the generalized Marcum's Q function, which is defined as

$$\begin{aligned} Q_m(a,b) &= \int_b^a x\left(\frac{x}{a}\right)^{m-1}\exp\left(-(\frac{x^2+a^2}{2})\right)I_{m-1}(ax)dx \\ &= Q_1(a,b) + \exp\left(-(\frac{x^2+a^2}{2})\right)\sum_{k-1}^{m-1}\left(\frac{b}{a}\right)^k I_k(ab) \end{aligned} \tag{5.50}$$

where

$$Q_1(a,b) = \exp\left(-\frac{x^2+a^2}{2}\right)\sum_0^{\infty}\left(\frac{b}{a}\right)^k I_k(ab), \qquad b > a > 0 \tag{5.51}$$

As what we discuss above, the received power follows a non-central chi-square distribution, we introduce random power allocation following inverted non-central chi-square distribution to mitigate the channel fading (Elmusrati et al. 2007}. Let $f_P(p)$

and $F_P(p)$ be the PDF and CDF of the random power respectively. Then we can obtain the inverted distribution of $f_P(p)$ (Elmusrati et al. 2007; Lehmann & Shaffer 1988) as

$$f_P(p) = \frac{1}{2p^2\sigma^2}\exp\left(-\frac{m^2+1/p}{2\sigma^2}\right) I_0\left(\sqrt{1/p}\,\frac{m}{\sigma^2}\right), \qquad p \geq 0 \tag{5.52}$$

and the CDF becomes

$$F_{P_{ij}}(p) = Q_1\left(\frac{m}{\sigma}, \frac{\sqrt{1/p}}{\sigma}\right) \tag{5.53}$$

Practically, the transmit power should be constrained to $p_{min} \leq p \leq p_{max}$. For the sake of simplicity, we assume $p_{\min} = 0$, then $F_P(p_{min}) = F_P(0) = 0$. Now we can obtain the truncated PDF as following

$$f_P(p) = \begin{cases} \dfrac{1}{2 \cdot F_P(p_{max}) \cdot p^2\sigma^2}\exp\left(-\dfrac{m^2+1/p}{2\sigma^2}\right) \cdot I_0\left(\sqrt{1/p}\,\dfrac{m}{\sigma^2}\right), & p_{\max} \geq p \geq 0 \\ 0, & \textit{others} \end{cases} \tag{5.54}$$

This PDF will be used to generate the random power for each time slot.

Let $R_{ij} = G_{ij}P_j$ denote the received power at receiver i transmitted by transmitter j. In this case, the transmit power P_j is random, which has the PDF and CDF, $f_P(p)$ and $F_P(p)$ respectively. Therefore the characteristic function of the received power $\Psi_{R_{ij}}$ can be given by

$$\Psi_{R_{ij}}(s) = \int_0^\infty \Psi_{G_{ij}}(ps) f_P(p) dp \tag{5.55}$$

Let us define a new normalized variable

$$\beta_i = \frac{\gamma_i \left(I_i + N_i^2 \right)}{g_i p_i} = \frac{\gamma_i \left(\sum_{i \neq j} G_{ij} P_j + N_i^2 \right)}{g_i p_i} \tag{5.56}$$

Then the characteristic function for β_i becomes

$$\Psi_{\beta_i}(\omega) = \prod_{j \neq i} \Psi_R \left(w \frac{\gamma_i g_{ij}}{g_i} \right) \exp\left(\frac{\gamma_i N_i^2}{g_i} \right) \tag{5.57}$$

Thus the probability of outage can be calculated as following

$$Pr\left\{ G_i P_i \leq \gamma_i \left(I_i + N_i^2 \right) \right\} = \int_0^\infty F_G(\beta) f_{\beta_i}(\beta) d\beta \tag{5.58}$$

where $f_{\beta_i}(\beta)$ can be obtained by using inverse-Fourier transform to the characteristic function $\Psi_{\beta_i}(\omega)$.

5.6.2 Numerical Results

We assume there are 24 users randomly distributed around the base station with a distance from 30 to 200 meters. The distance exponent factor is 4, and the noise power is fixed at -70dBm. The log-normal shadow fading has a 0dB mean and 6dB variance. The random transmit power of the user in each time slot is produced by transform method according to equation 5.54. We do not consider the processing gain and the target SINR is $E_b / N_0 = 7\text{dBm}$. The procedure of calculating the average the outage probability is repeated 300 times.

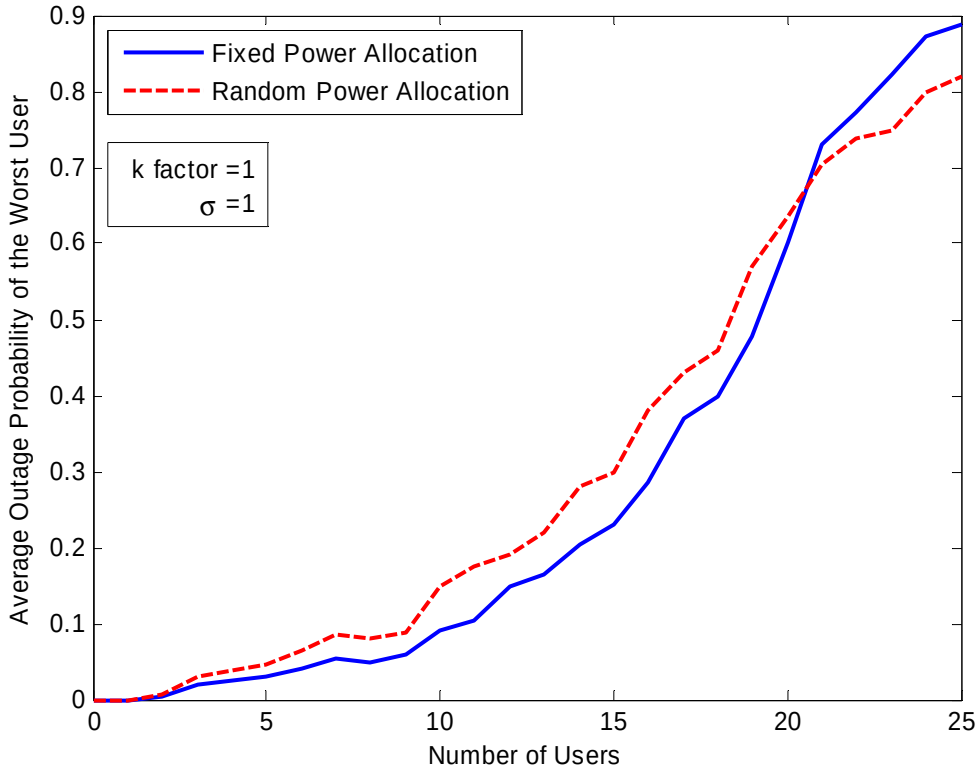

Figure 5.9: Simulated Average Outage Probability of the Worst User with Respect to the Number of Users.

Fig. 5.9 shows the average of the all the users added to the system. In this simulation the procedure of calculating the average the outage probability is repeated 300 times, Ricain factor $k = 1$, and the multipath standard variance is 1. Also, the users are added to the system one by one from the furthest to the nearest. When the number of users increases, the outage probability will increase.

In this section, the uncorrelated Rician fading channel is considered where the current channel measurement information is useless for power control updating. We utilize and analyze the random power allocation at the terminal where the transmit power is generated for each time slot following the probability density function (5.54). Also the

truncated inverted non-central chi-square distribution is used for generating random power.

In the future work, the comparison between presented power control scheme and conventional DPC algorithm should be added. Also the average transmit power between these schemes should be presented.

6. CONCLUSION AND FUTURE WORK

In this thesis, we discussed the essential characteristics of time-varying wireless channels. The time variations as well as time delays between the channel measurements and resource allocation reduce the performance of current radio resource management (RRM) algorithms. We also discussed by using simple examples that radio RRM is one of the most important parts of modern multi-user wireless communication systems, and also that the optimal radio resource allocation guarantees the efficient utilization of wireless networks. To optimize the radio resources, the transmitters need to estimate the channel conditions. This channel estimation is done by using pilot signal from the receiver. However, there are usually small delays between the measurements and the radio resource allocation. When the channel is highly correlated, this delay does not affect the performance, because the channel has not significantly changed between the time of measurement and that of transmission. However, if the mobile speed is high or the channel is very high dynamic, the time correlation becomes very low. This is due to the time-varying nature of the channel. Consequently, we named channels with very low correlation in time as bad condition channels.

Different concepts of wireless channels have been presented in this report. First, the conventional radio wave transmission techniques were illustrated. In this part we discussed the free space, shadowing, and multipath channels. Second, the time-varying characteristics of multipath fading were discussed. Several important concepts on probability and stochastic process have been introduced. Those are important for analyzing the time-varying multipath fading channels. Moreover, we have presented several quite important concepts: flat fading (or non frequency selective fading), frequency selective fading, fast fading, and slow fading, and the essential differences among them. They are, as following:

- The multipath delay spreading determines whether a signal undergoes flat fading or frequency selective fading.

• The time variation or Doppler spread, which depends on the motion of the mobile or objects in the channel, determines whether a signal undergoes fast fading or slow fading.

Power control concepts were presented. The importance of power control in multi-user CDMA systems were demonstrated via numerical examples. The centralized as well as distributed power control schemes were given.

Finally, we proposed two power control schemes for bad channel conditions: DPC based on channel correlation for low correlated channels and random power allocation for uncorrelated Rician fading channels. Besides the theoretical analysis of our proposed algorithms, we have presented several results based on simulations. Simulations show that the modified DPC algorithm which considers the channel correlation has better performance than the conventional DPC algorithm in terms of average outage. However, the random power allocation has not improved the average performance of the system. It has improved only the worst-channel terminals. This needs more investigations to improve the results.

For future research work, we will consider other radio resources such as bandwidth, time, handover, beamforming as well. The optimizing of such resources in bad channel conditions will be our main target. Several tools are expected to be used such as advanced stochastic tools, multi-objective optimization, and game theory.

BIBLIOGRAPHY

Ahmed, H. Mohamed and Mahmoud Elsayes (2007). *Accurate Upper Bound of SINR-based Call Admission Threshold in CDMA Systems with Imperfect Power Control*. IEEE Comm. letters, vol. 11, No. 3, 258-260.

Almgren, Magnus, Hkan Andersson and Kenneth Wallstedt (1994). *Power Control in Cellular Systems*. Proc. IEEE Veh. Tech. Conf., VTC-94, 833-837.

Amitay, Noach (1992). *Modeling and Computer Simulation of Wave Propagation in Lineal Line-of-sight Microcells*. IEEE Trans. Veh. Tech., Vol VT-41, No. 4, 337-342.

Aulin, Tor (1981). *Characteristics of a Digital Mobile Radio Channel*. IEEE Trans. Veh. Technol., vol. VT-30, 45-53.

Bello, Philip (1963). *Characterization of Randomly Time-variant Linear Channels*. IEEE Trans. Commun. Syst., vol. CS-11, No. 4, 360-393.

Charash, Rafael U. (1979). *Reception Through Nakagami Fading Multipath Channels with Random Delays*. IEEE Trans. Commun., Vol. 27, 657-670.

Clarke, Richard H. (1968). *A Statistical Theory of Mobile-radio Reception*. Bell Syst. Tech. J., vol. 47, 957-1000.

Elmusrati, Mohammed S. (2004). *Radio Resource Scheduling and Smart Antennas in Cellular CDMA Communication Systems*. Doctoral Thesis, Helsinki University of Technology, Control Engineering Laboratory, Report 142.

Elmusrati, Mohammed S. and Heikki N. Koivo (2002). *Multi-objective Distributed Power Control Algorithm*. IEEE 56th Vehicular Technology Conference

Proceedings, vol.2, 812- 816.

Elmusrati, Mohammed S., Naser Tarhuni and Riku Jäntti (2007). *A Framework for Random Power Allocation of Wireless Networks in Rayleigh Fading Channels*. IEEE transactions on wireless communications. submitted manuscript.

Foschini, Gerard J. and Zoran Miljanic (1993). *A Simple Distributed Autonomous Power Control Algorithm and its Convergence*. IEEE Trans. Veh. Tech., vol. 42 641-646.

Gans, Michael J. (1972). *A power Spectral Theory of Propagation in the Mobile Radio Environment*. IEEE Trans. Veh. Tech., vol. VT-21, No. 1.

Gantmacher, Felix R. (1964). *The Theory of Matrices*. vol. 2. New York: Chelsea Publishing Company.

Giancristofaro, Domenico. (1996). *Correlation Model for Shadow Fading In Mobile Radio Systems*. IEEE Electronics Letters, Vol. 32, No. 11, 958-959.

Goldsmith, Andrea (2005). *Wireless Communications*. Cambridge: Cambridge University Press.

Goldsmith, Andrea (1994). *Design and Performance of High-Speed Communication Systems over Time-Varying Radio Channels*. Ph.D. dissertation: Dept. Elec. Eng. Comput. Sci., Univ. California, Berkeley.

Grandhi, Sudheer A., Rajiv Vijayan, David J. Goodman and Jens Zander (1993). *Centralized Power Control for Cellular Radio Systems*. IEEE Transactions on Vehicular Technology, No. 42.

Grandhi, Sudheer A., Rajiv Vijayan and David J. Goodman (1994). *Distributed Power Control in Cellular Radio Systems*. IEEE Trans. on Comm. vol. 42, No. 2.

Grandhi, Sudheer A., Jens Zander and Roy Yates (1995). *Constrained Power Control*. Wireless Personal Communications, vol. 2, No. 3.

Gudmundson, Mikael (1991). *Correlation Model for Shadow Fading In Mobile Radio Systems*. IEEE Electronics Letters, 27(23): 2145-2146.

Gunnarsson, Fredrik, Fredrik Gustafsson and JonasBlom (2001). *Dynamical Effects of Time Delays and Time Delay Compensation in Power Controlled DS-CDMA*. IEEE J. Select. Areas Commun., vol. 19.

Harry, Holma and Antti Toskala (2000). *WCDMA for UMTS: Radio Access for Third Generation Mobile Communications*. New York: John Wiley & Sons.

Hasu, Vesa (2007). *Radio Resource Management in Wireless Communication: Beamforming, Transmission Power Control, and Rate Allocation*. Doctoral Thesis, Helsinki University of Technology, Signal Processing Laboratory, Report 152.

Holliday, Tim, Nick Bambos, Peter Glynn, Andrea Goldsmith (2003). *Distributed Power Control for Time Varying Wireless Networks: Optimality and Convergence*. Proc. Allerton Conf. Communications, Control, Computing, Monticello, IL.

Jakes, William C. (1993). *Microwave Mobile Communications*. New York: IEEE Press.

Jäntti, Riku. (2001). *Power control and Transmission Rate Management in Cellular Radio Systems*. Doctoral Thesis, Helsinki University of Technology, Control Engineering Laboratory, Report 123.

Jäntti, Riku and Seong-Lyun Kim (2000). Second-*Order Power Control with Asymptotically Fast Convergence*. IEEE Selected Areas of Communications, vol. 18, No. 3, 447-457.

Jeruchim, Michel C., Philip Balaban and K. Sam Shanmugan (2000). *Simulation of Communication Systems: Modeling, Methodology, and Techniques*. 2nd Ed. New York: Kluwer Academic/Plenum Press.

Karasawa, Yoshio and Hisato Iwai (1994). *Modeling of Signal Envelope Correlation of Line-of-Sight Fading with Applications to Frequency Correlation Analysis.* IEEE Trans. Commun., vol. 42, 2201-2203.

Kim, Tae-Suk and Seong-Lyun Kim (2005). *Random Power Control in Wireless Ad hoc Networks*. IEEE Comm. Letters, Vol.9, No.12, 1046-1048.

Lee, William C. Y. (1982). *Mobile Communications Engineering*. 2nd Ed. New York: McGraw-Hill.

Lee, HyeJeong and Dong-Ho Cho (2003). *A New User Mobility Based Adaptive Power Control in CDMA Systems.* IEICE Trans. Commun., E86-B, No. 5, 1702-1705.

Lee, Geun-Joon and Sang C. Park (2002). *Distributed Power Control in Fading Channel.* IEEE Elec. Letters, vol. 38, 653-654.

Lehmann, Eric L. and Juliet P. Shaffer (1988). *Inverted distributions.* American Statistician, Vol.56, 191-194.

Lindsey, WILLIAM. C. (1964). *Error Probabilities for Rician Fading Multichannel Reception of Binary and N-ary Signals*. IEEE Trans. Inf. Theory, vol. IT-10, No. 4, 339-350.

Mathworld (2008). *Iterative Methods* [online]. [cited 6 March 2008]. <URL: http://mathworld.wolfram.com/topics/IterativeMethods.html>.

Nakagami, Masaki (1960). *The m-distribution: A General Formula of Intensity Distribution of Rapid Fading, in Statistical Methods in Radio Wave Propagation.* W. G. Hoffman, Ed. Oxford, U.K., Pergamon, 3-36.

Neto, Raimundo A. de O., Tarcisio F. Maciel, Francisco R. P. Cavalcanti and Fabiano S. Chaves (2004). *Distributed Power Control with Tracking of Fast Fading and Interference*. Proc. of the IEEE Semiannual Veh. Tech. Conf. (VTC2004-Spring), Milan, Italy.

Nielsen, P. Tolstrup (1978). *Mean Power of the Components of a Rice Fading Signal Determined from Measurements*. Proceedings of the IEEE, Vol. 66, No. 9.

Papoulis, Athanasios (1965). *Probability, Random Variables and Stochastic Processes*. New York: McGraw-Hill.

Parsons, John David (1999). *The mobile radio propagation channel*. New York: Addison-Wesley.

Peritsky, Martin M. (1973). *Statistical Estimation of Mean Signal Strength in a Rayleigh Fading Environment.* IEEE Trans. Commun., vol. COM-21, 1207-1213.

Peritsky, Martin M. (1976). *Correction to Statistical Estimation of Mean Signal Strength in a Rayleigh Fading Environment.* IEEE Trans Veh. Technol., vol. VT-25, 92.

Pristinsky, Andrey (2002). *Radio Resource Management across UMTS Radio Network Subsystems*. Master's Thesis, Lappeenranta University of Technology.

Proakis, John G. (2000). *Digital Communications.* 4th Ed. New York: McGraw-Hill.

Rappaport, Theodore S. (2002). *Wireless Communications principles and practice.*

2nd Ed. New Jersey: Prentice Hall.

Schaubach, Kurt R., Nathaniel J. Davis IV and Theodore S. Rappaport (1992). *A Ray Tracing Method for Predicting Path Loss and Delay Spread in Microcellular Environments*. Proc. IEEE Veh. Tech. Conf., 932-935.

Shepherd, William L. and Paul Milnarich (1937). *Basic Relations Between a Rayleigh-Distributed Randomly Varying Voltage and a Decibel Record of the Voltage.* Proc. IEEE, 1765-1766.

Sim, Moh Lim, Erry Gunawan, Cheong-Boon Soh and Boon-Hee Soong (1998). *Characteristics of Closed Loop Power Control Algorithms for a Cellular DS/CDMA System.* in Proc. Inst. Elect. Eng. Comm., vol. 147.

Sklar, Bernard (1997a). *Digital Communications: Fundamentals and Applications. 2nd Ed.* New Jersey: Prentice Hall, 2001.

Sklar, Bernard (1997b). *Rayleigh Fading Channels in Mobile Digital Communication Systems Part I*: Characterization. IEEE Communications Magazine.

Sklar, Bernard (1997c). *Rayleigh Fading Channels in Mobile Digital Communication Systems Part II*: Characterization, IEEE Communications Magazine.

Stüber, L. Gordon (2002). *Principles of Mobile Communications.* 2nd Ed. New York: Kluwer Academic.

Tjhung, T.Tjeng and Chin C. Chai (1999). *Fade Statistics in Nakagami-lognormal Channels*. IEEE Trans. Comm., Vol. 47, No. 12, 1769-1772.

Tse, David and Pramod Viswanath (2005). *Fundamentals of Wireless Communication. Cambridge University Press.* Cambridge: Cambridge University Press.

Ulukus, Sennur and Roy D. Yates (1998). *Stochastic Power Control for Cellular Radio*

Systems. IEEE Trans. Commun. vol. 46(6): 784-798.

Uykan, Zekeriya, Riku Jäntti and Heikki N. Koivo (2000). *A PI-Power Control Algorithm for Cellular Radio Systems*. Proceedings of IEEE Internationa Symposium on Spread Spectrum Techniques and Applications, ISSSTA 2000, vol. 2, 782-785.

Weerackody, Vijitha (1995). *The Effect of mobile speed on the forward link of the DS-CDMA cellular system*. Communication Theory Mini-Conf. 147-151.

Youssef, Neji, Tsutoniu Munakata and Mitsuo Takeda (1996). *Fade statistics in Nakagami fading environments*. Proc. IEEE Int. Symp. Spread Spectrum Techniques Applications, Mainz Germany, 1244-1247.

Zander, Jens (1996). *Radio Resource Management-An Overview*, Proc. VTC'96, Atlanta, GA.

Zander, Jens (1992). *Distributed Cochannel Interference Control in Cellular Radio Systems.* IEEE Transactions on Vehicular Technology, vol. 41 No. 3, 305-311.